Particle Acceleration in Pulsed Power Driven Magnetic Reconnection Experiments

Jack W. D. Halliday (jack.halliday12@imperial.ac.uk)

Imperial College: J. D. Hare, L. G. Suttle, S. V. Lebedev, S. N. Bland, S. Parker, D. R. Russell, E. R. Tubman

Cornell University & Lebedev Institute: S. A. Pikuz and T. A. Shelkovenko.

Imperial College London

Multi-university Center for Pulsed-Power Driven High Energy Density Science

MAGPIE

Supported by EPSRC Grant No. EP/N013379/1, and by the US DOE Awards No. DE-F03-02NA00057, DE-SC-0001063, and DE-NA-0003764.

The MAGPIE Current Generator

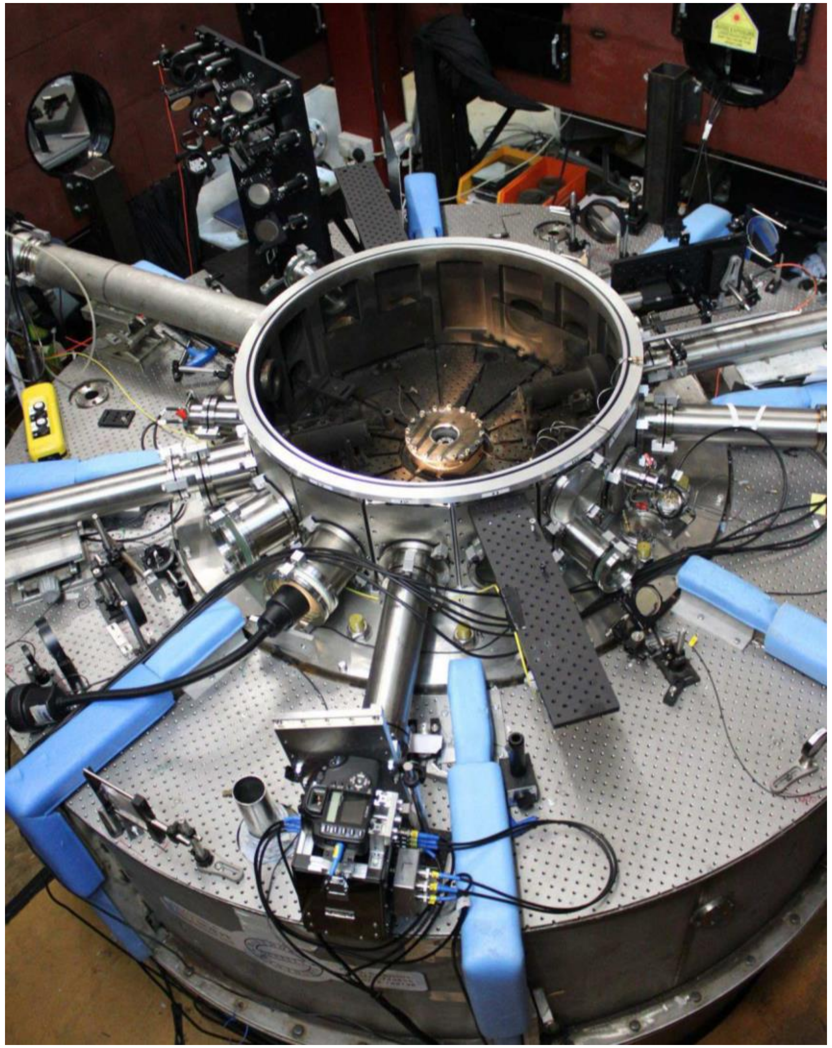

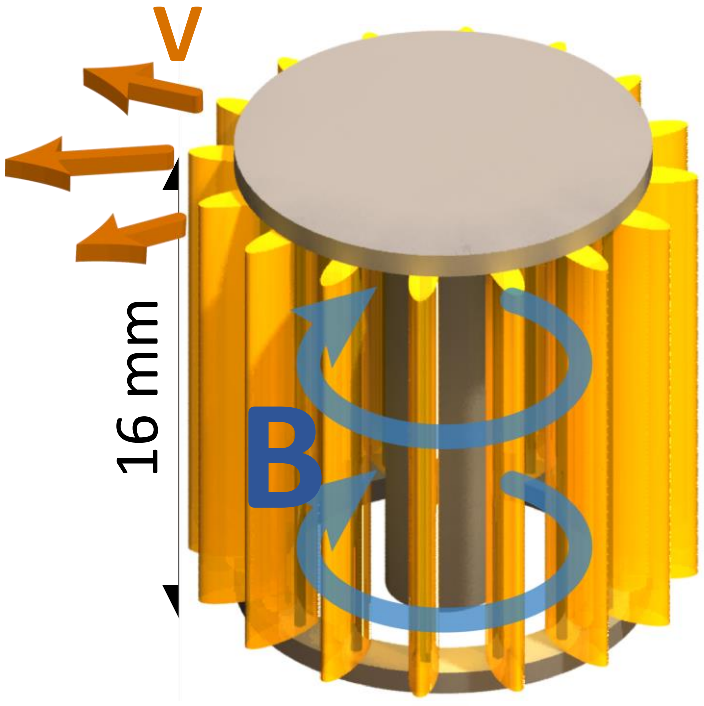

$t_{drive} \sim 500$ ns $\quad I_{peak} \sim 500$ ns

The MAGPIE Current Generator

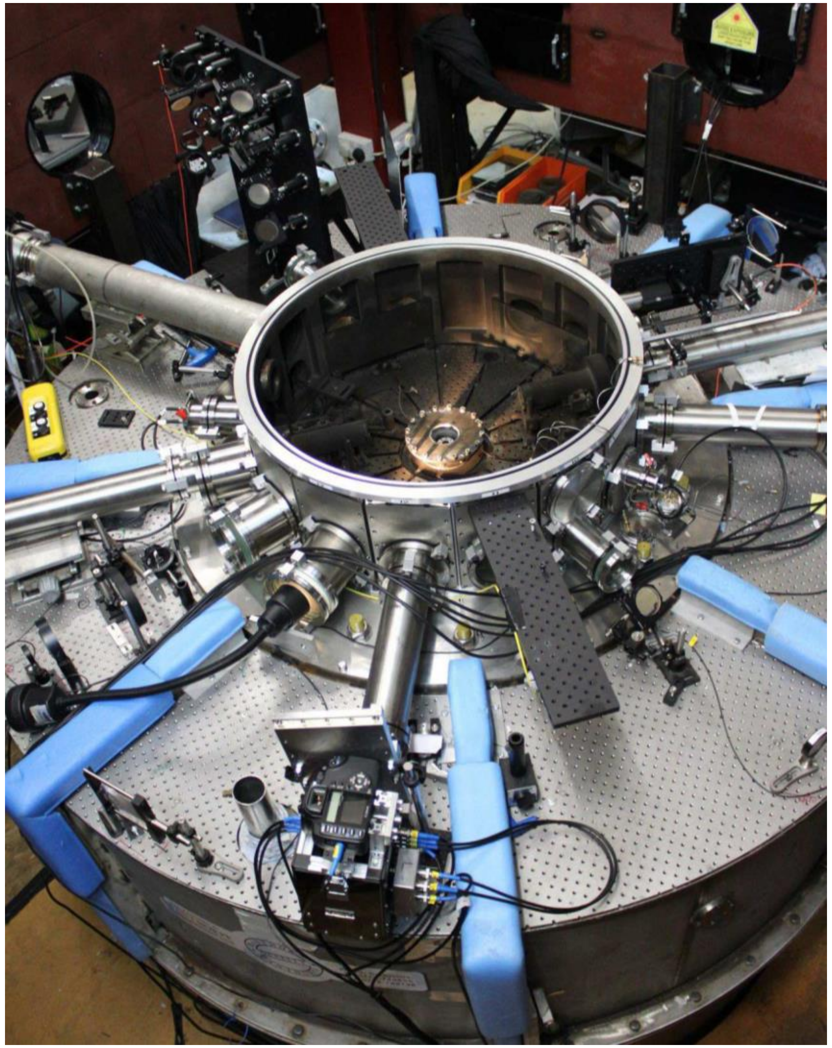

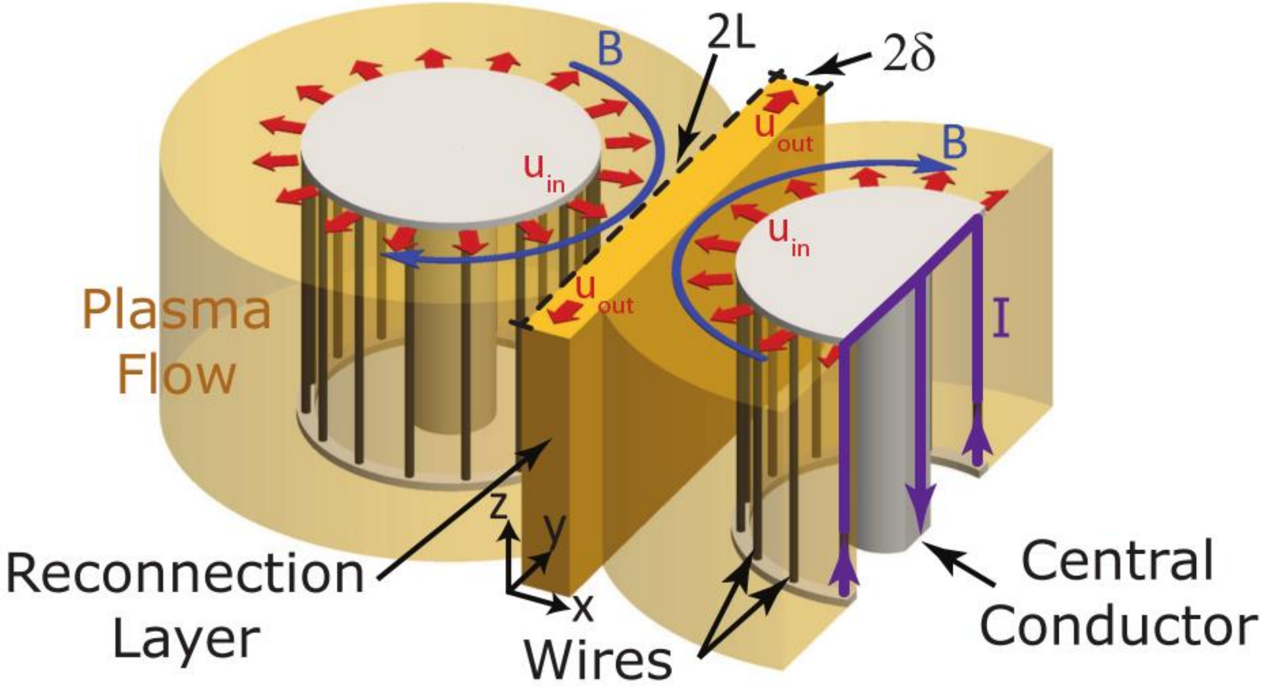

The MAGPIE Reconnection Framework

Parameter	Value
t_{drive}	500 ns
B_{in}	3 T
L/d_i	$\sim$20
S	$\sim$ 100
β	$\sim$ 1

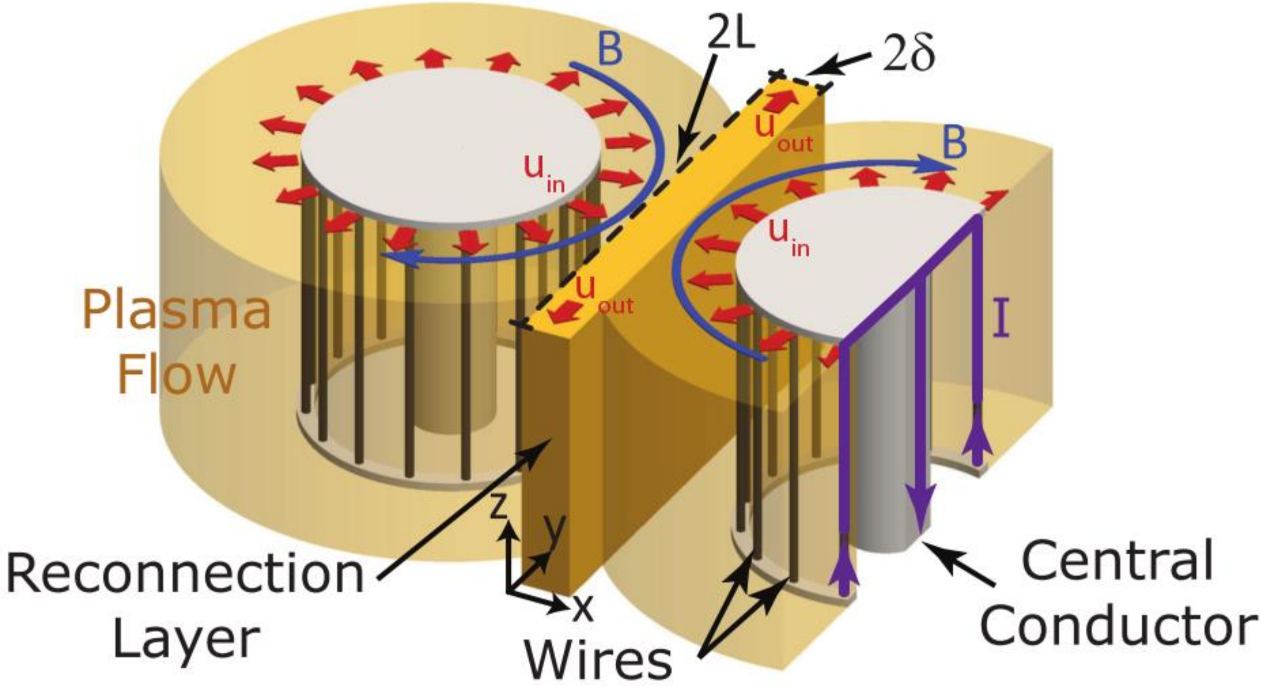

L. G. Suttle *et al.* – PRL 2016; PoP 2018

J. D. Hare *et al.* – PRL 2017; PoP 2017; PoP 2018

The Magnetic Reconnection Framework

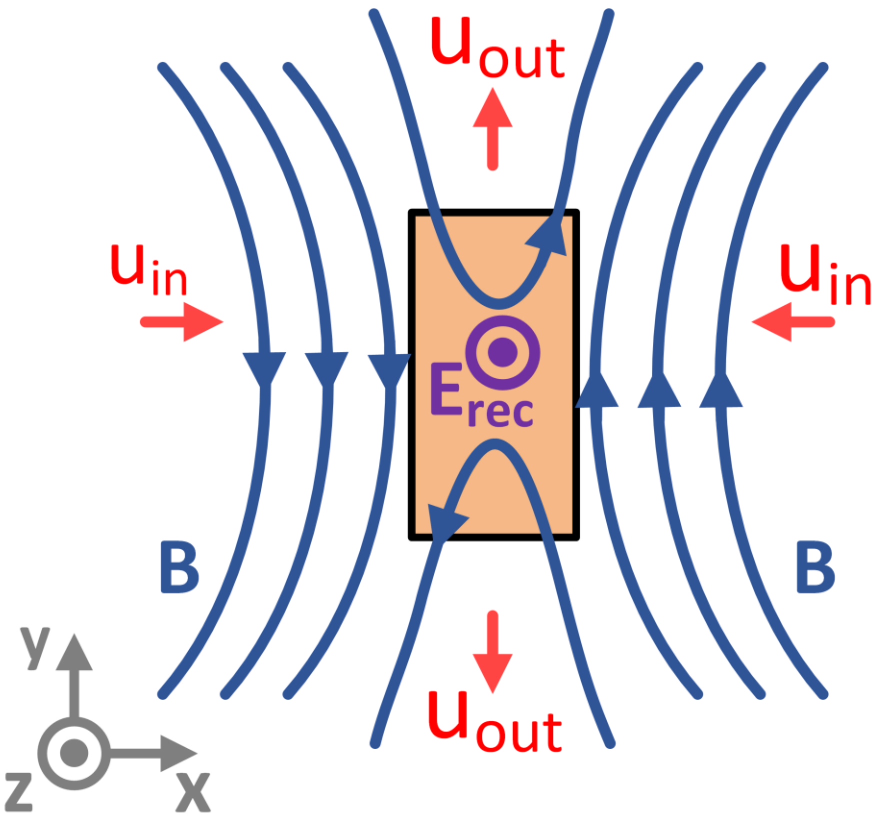

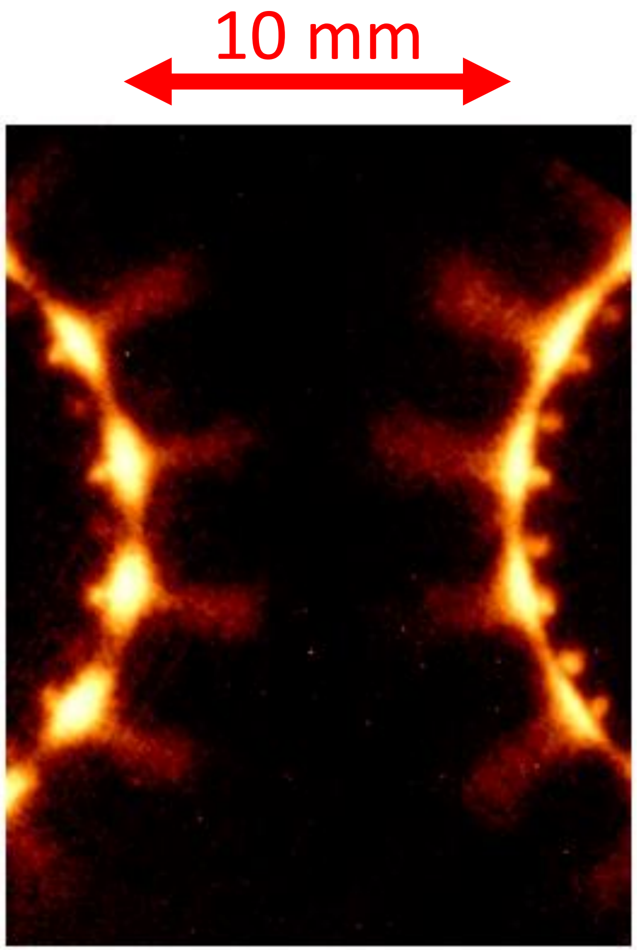

Electron Acceleration in Reconnection

End-On View (X-Y Plane)	Side-On View (X-Z Plane)

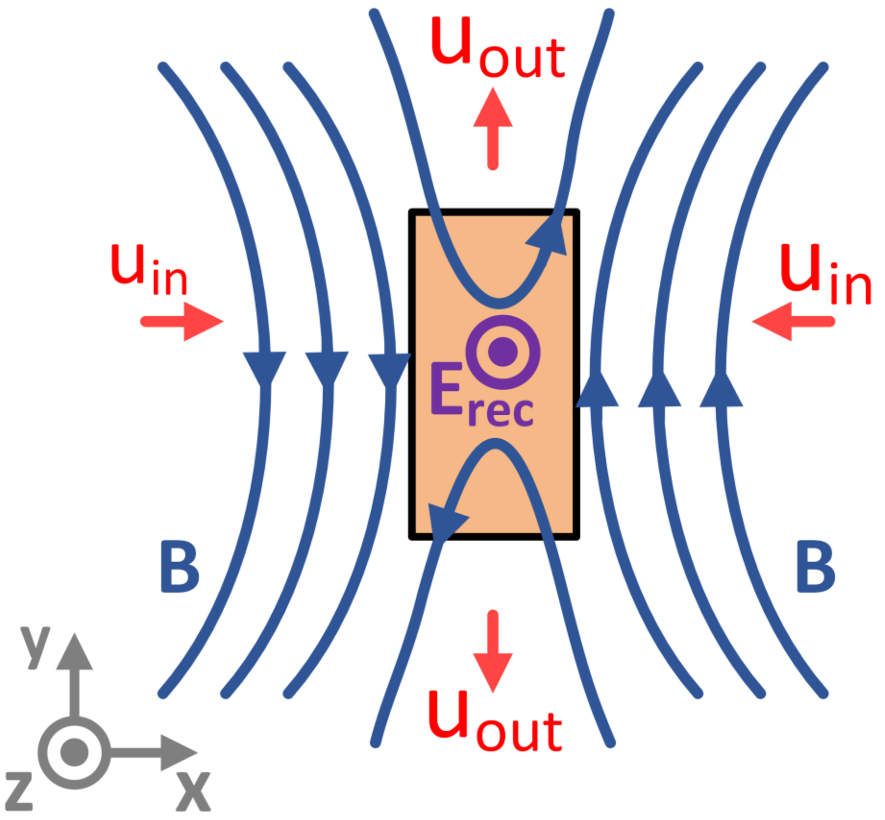

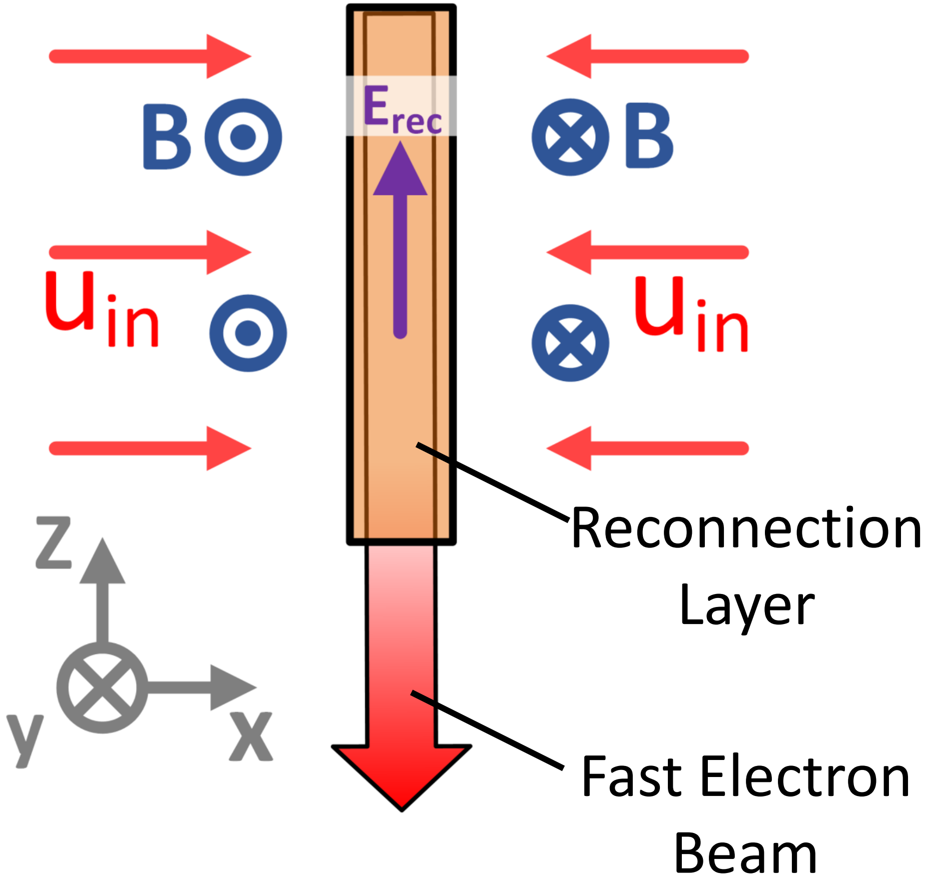

The Reconnecting Electric Field (E_{rec})

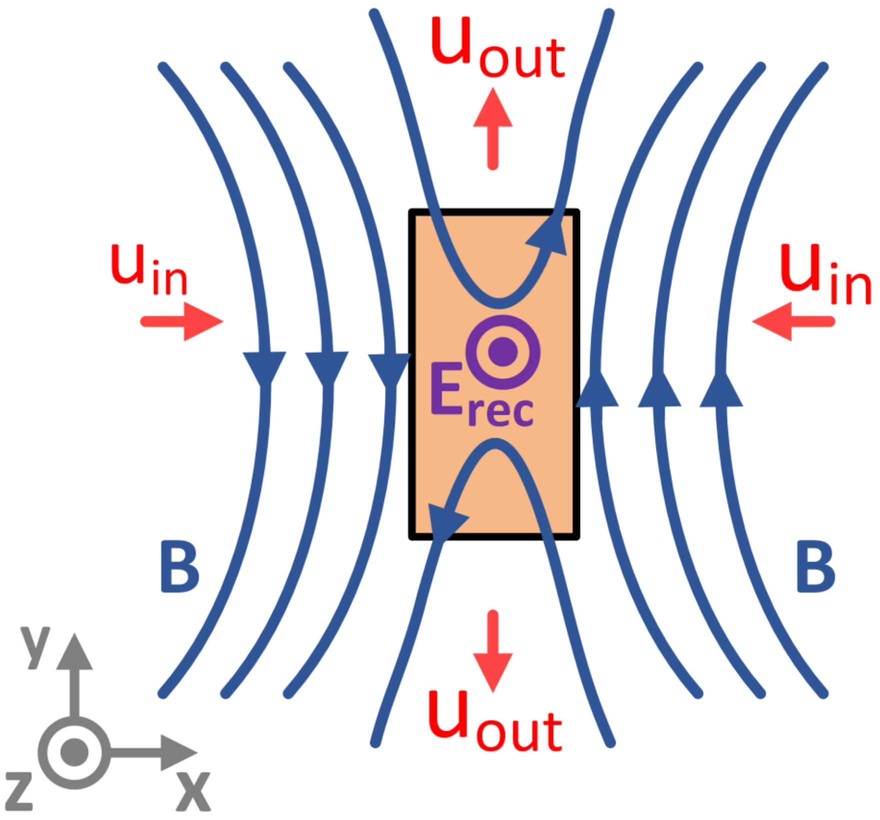

Parameter	Value	Diagnostic
u_{in}	$50\ \mathrm{km/s}$	Thomson Scattering
B_{in}	$3\ \mathrm{T}$	Faraday Rotation
L_z	$16\ \mathrm{mm}$	Interferometry

$$\mathbf{E} = -\mathbf{u} \times \mathbf{B} + \eta \mathbf{j}$$

$$E_{rec} = u_{in} B_{in} = 150\ \mathrm{kV/m}$$

$$\int \mathbf{F} \cdot d\mathbf{l} \sim e E_{rec} L_z = 2.4\ \mathrm{keV}$$

Diagnosing Fast Electrons

End-On View (X-Y Plane)

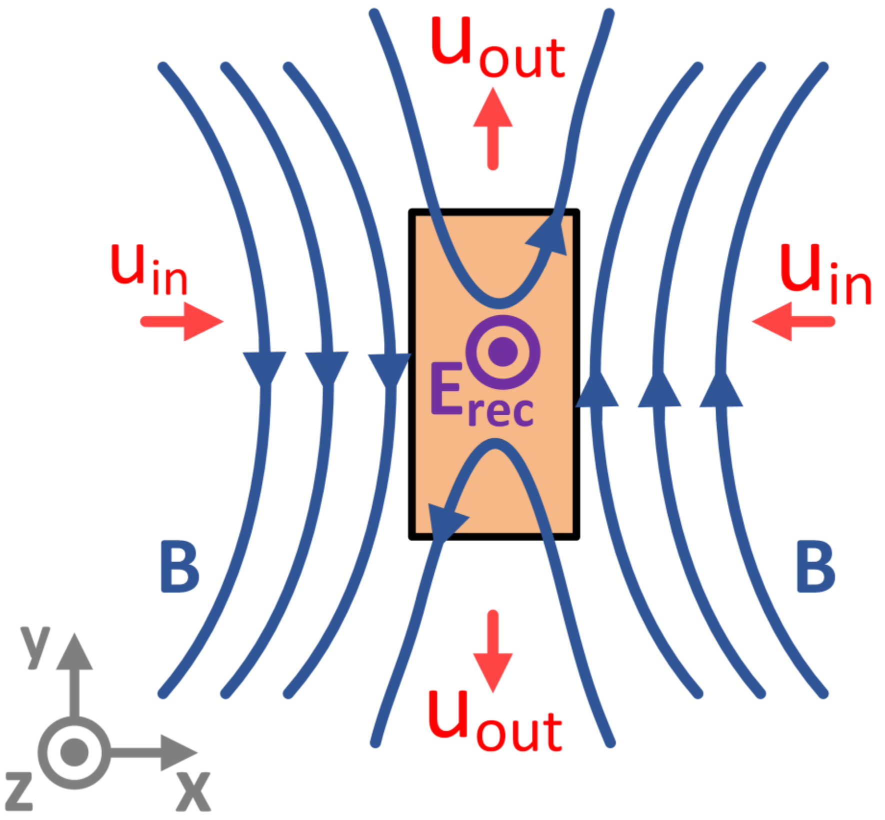

Side-On View (X-Z Plane)

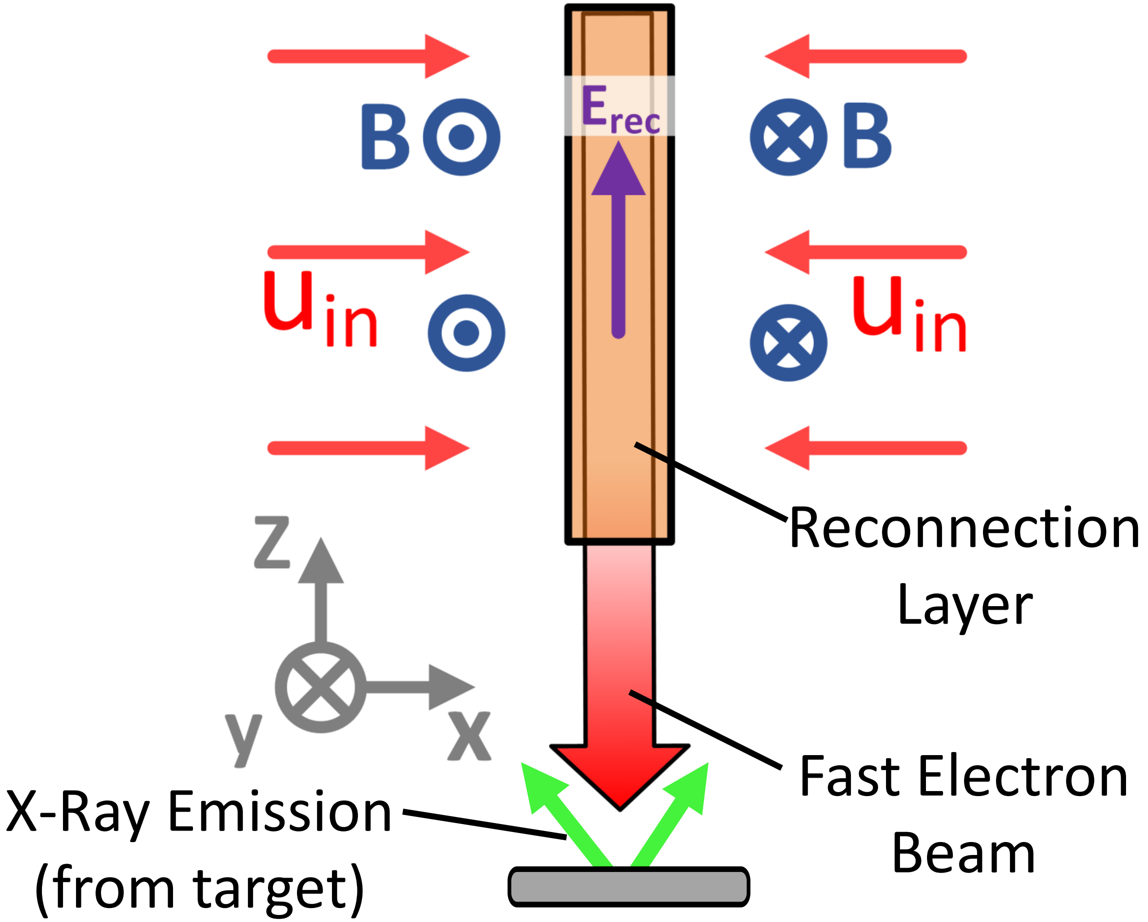

Diagnosing Fast Electrons

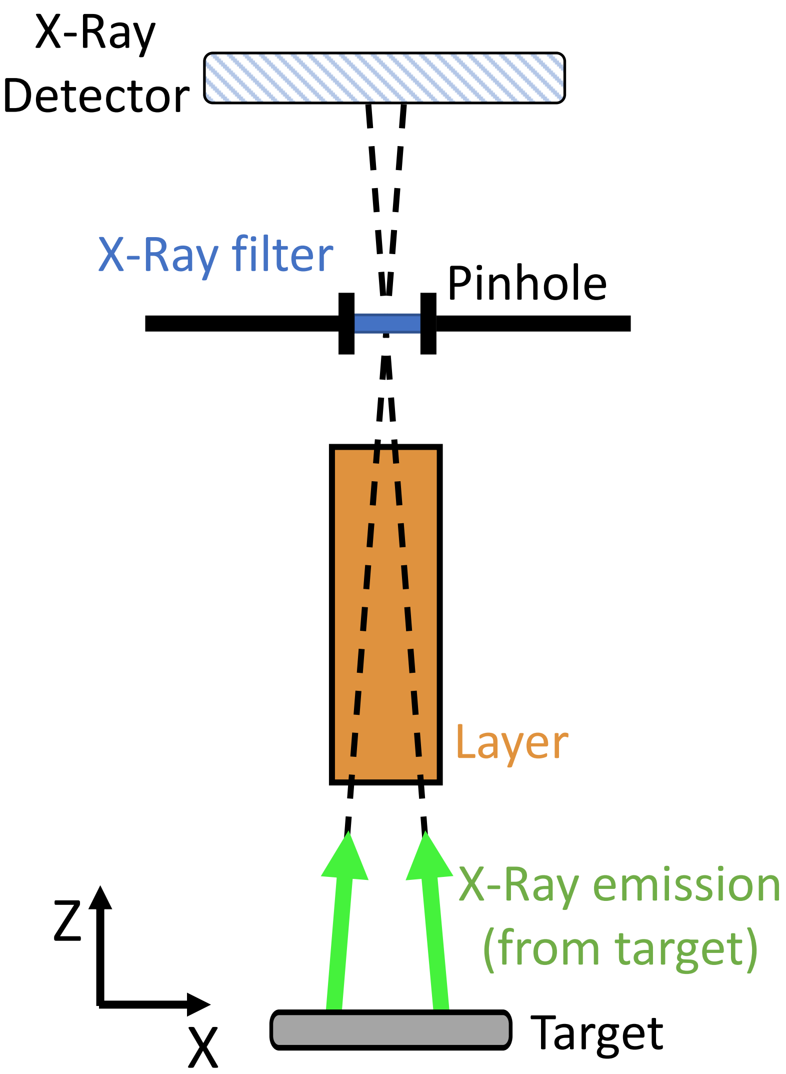

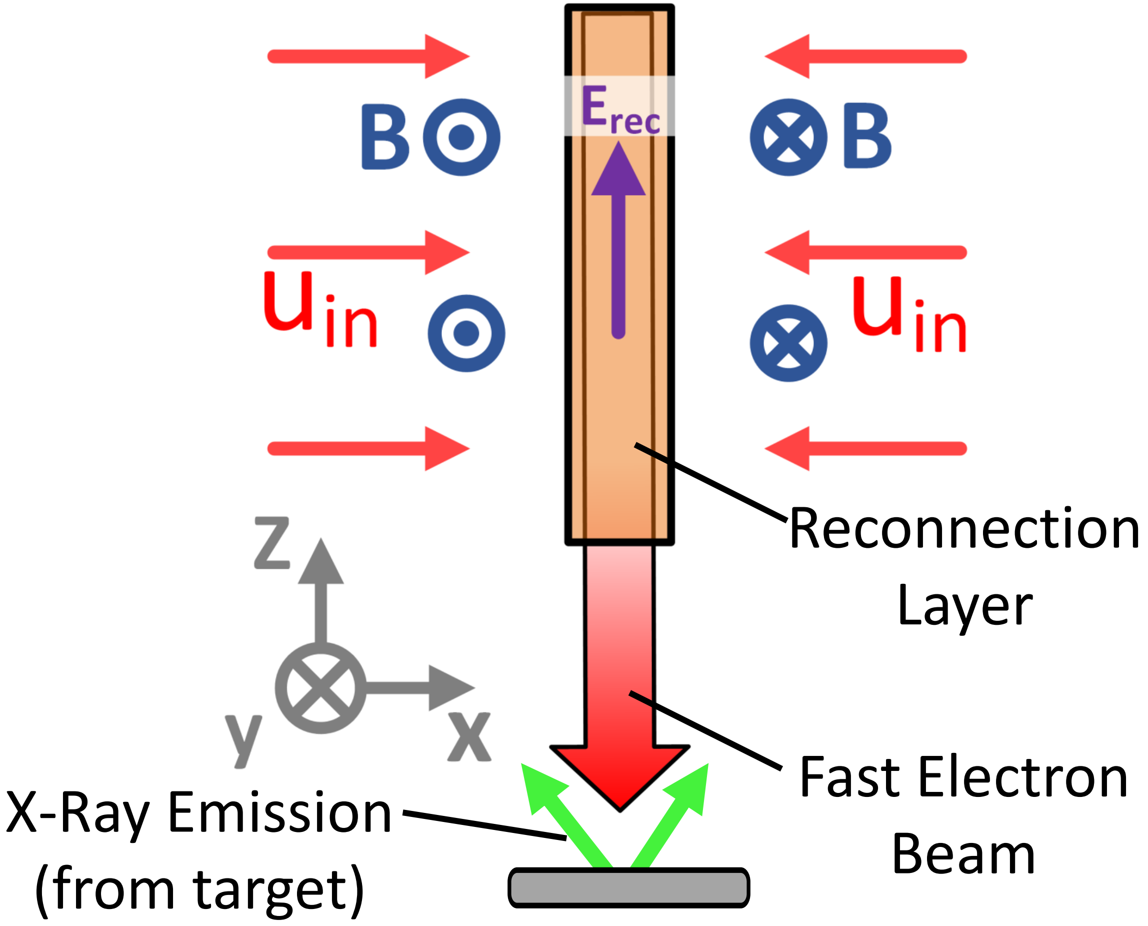

Time Integrated Pinhole Images

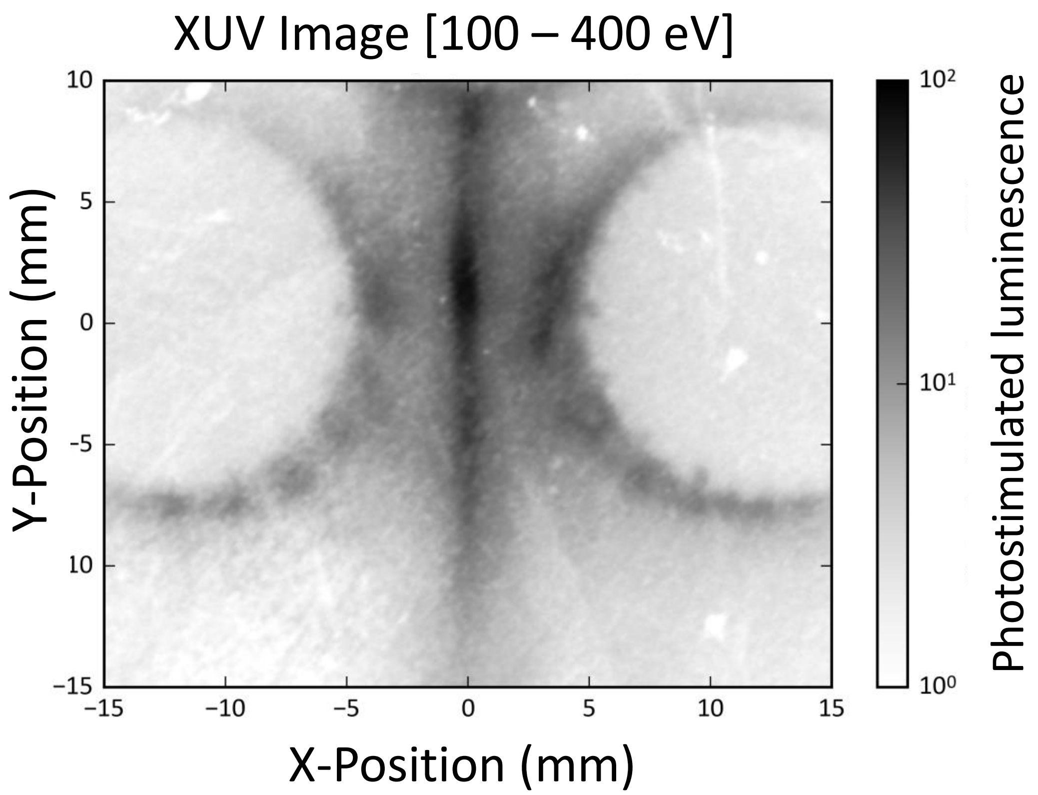

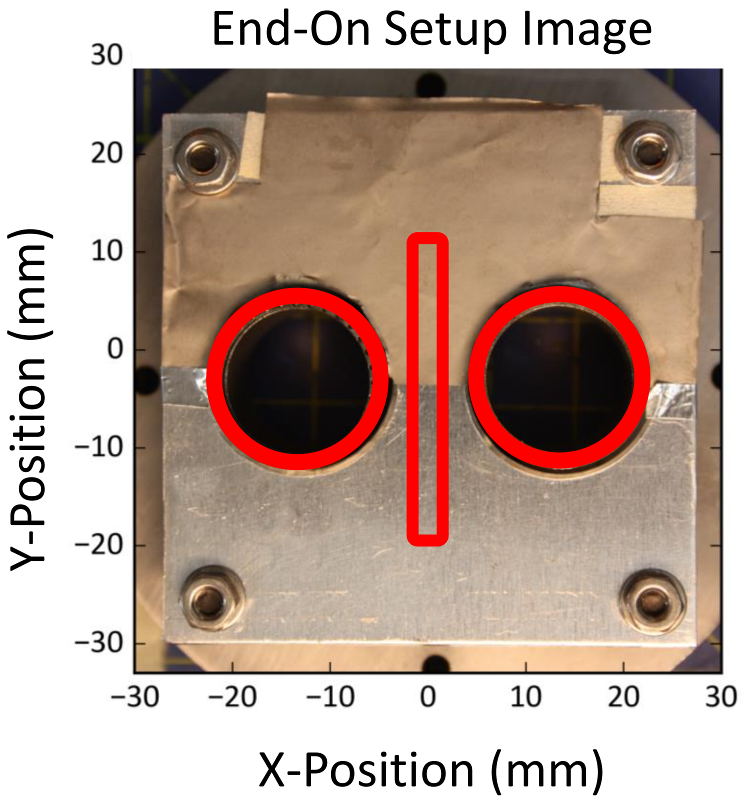

Thomson Scattering ⇒ $T_e \leq 100$ eV

Time Integrated Pinhole Images

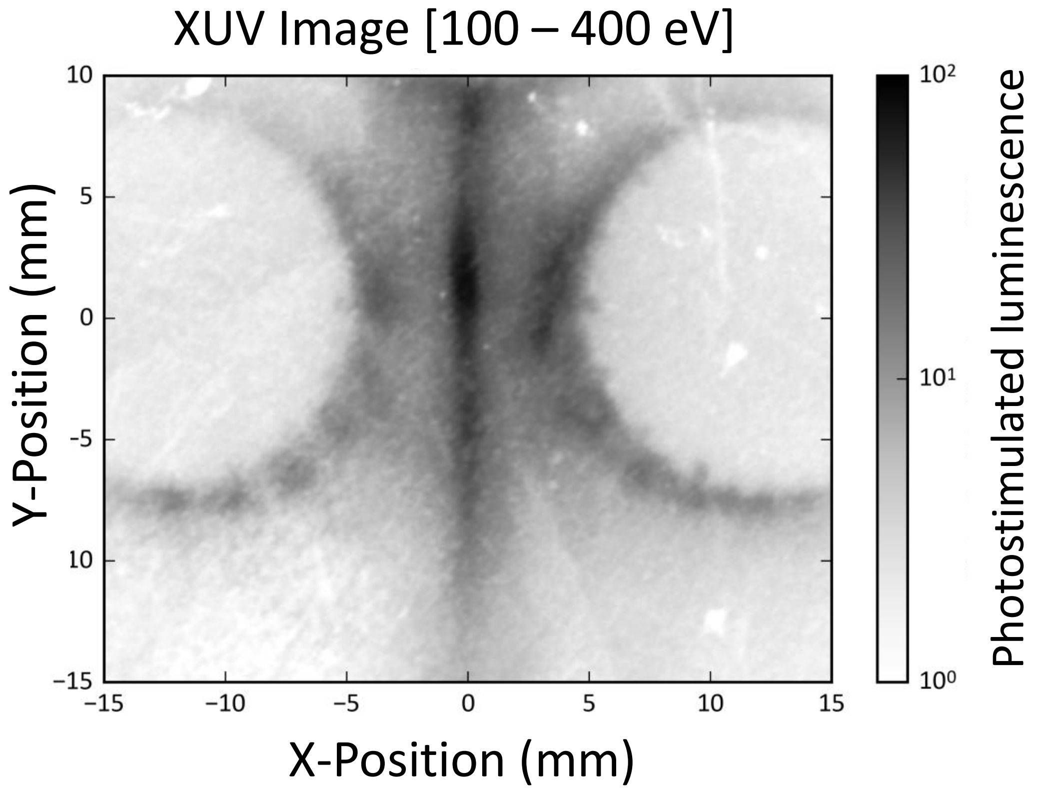

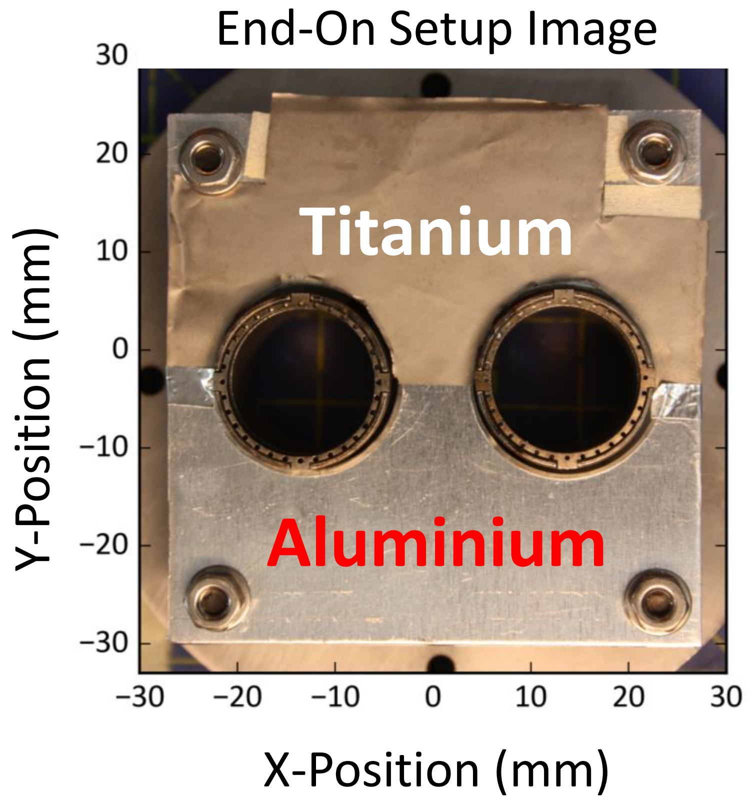

Thomson Scattering ⇒ $T_e \leq 100\ \mathrm{eV}$

Time Integrated Pinhole Images

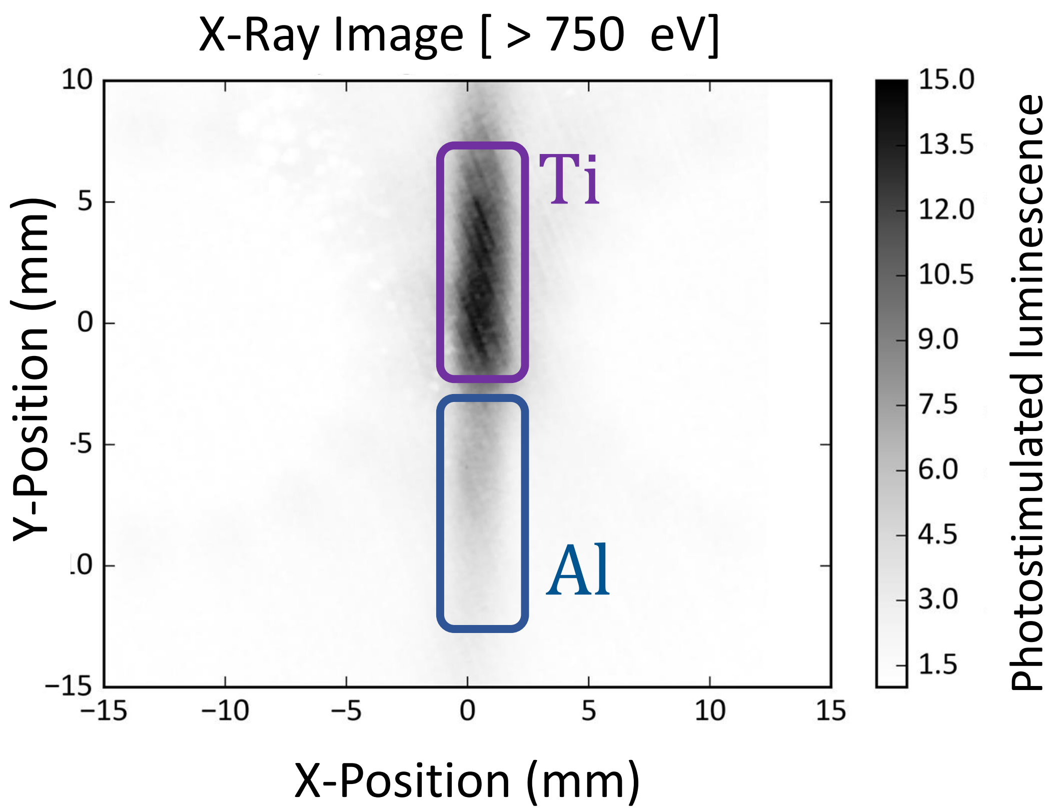

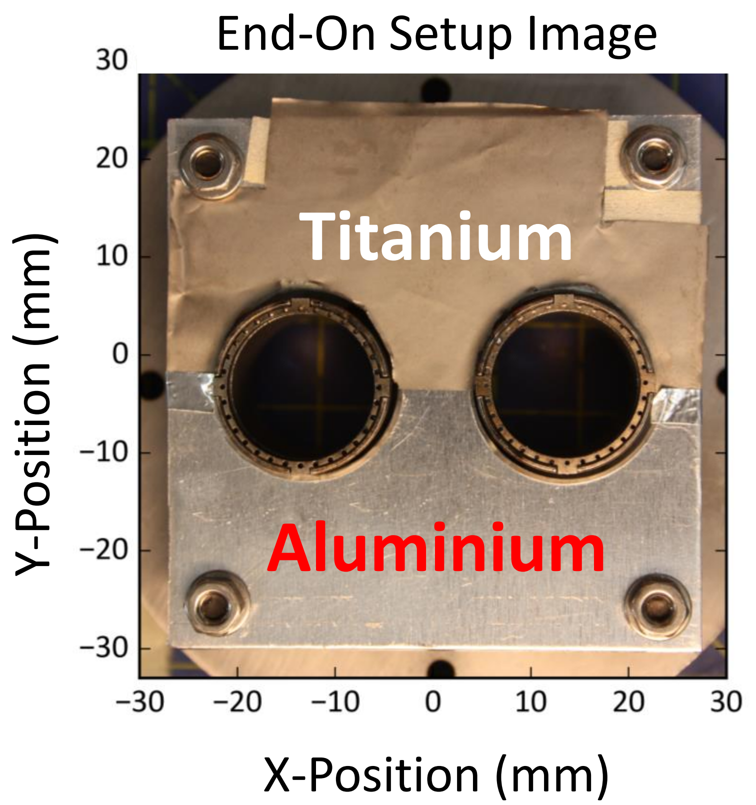

Thomson Scattering ⇒ $T_e \leq 100$ eV

Time Resolved X-Ray Imaging Data

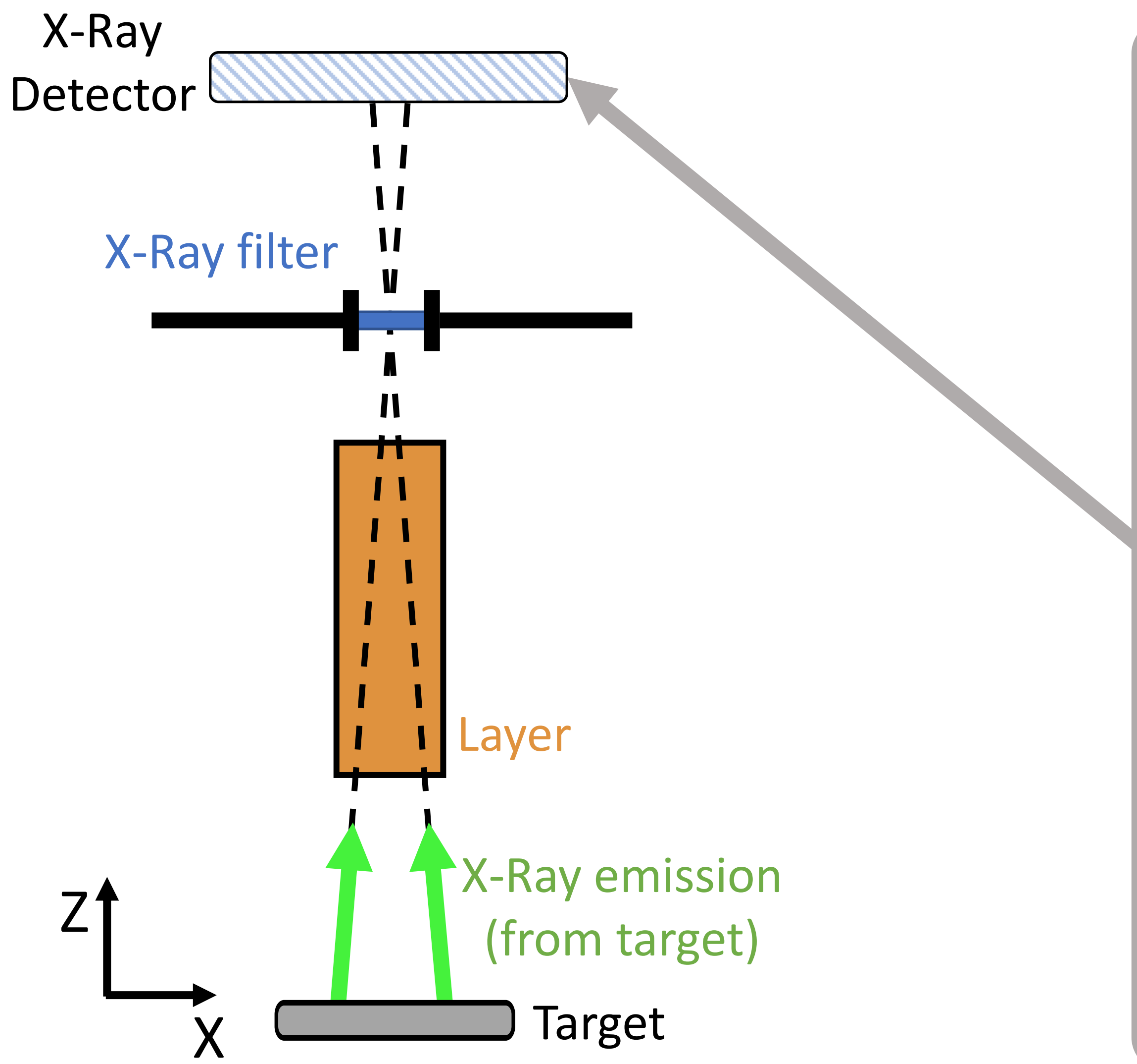

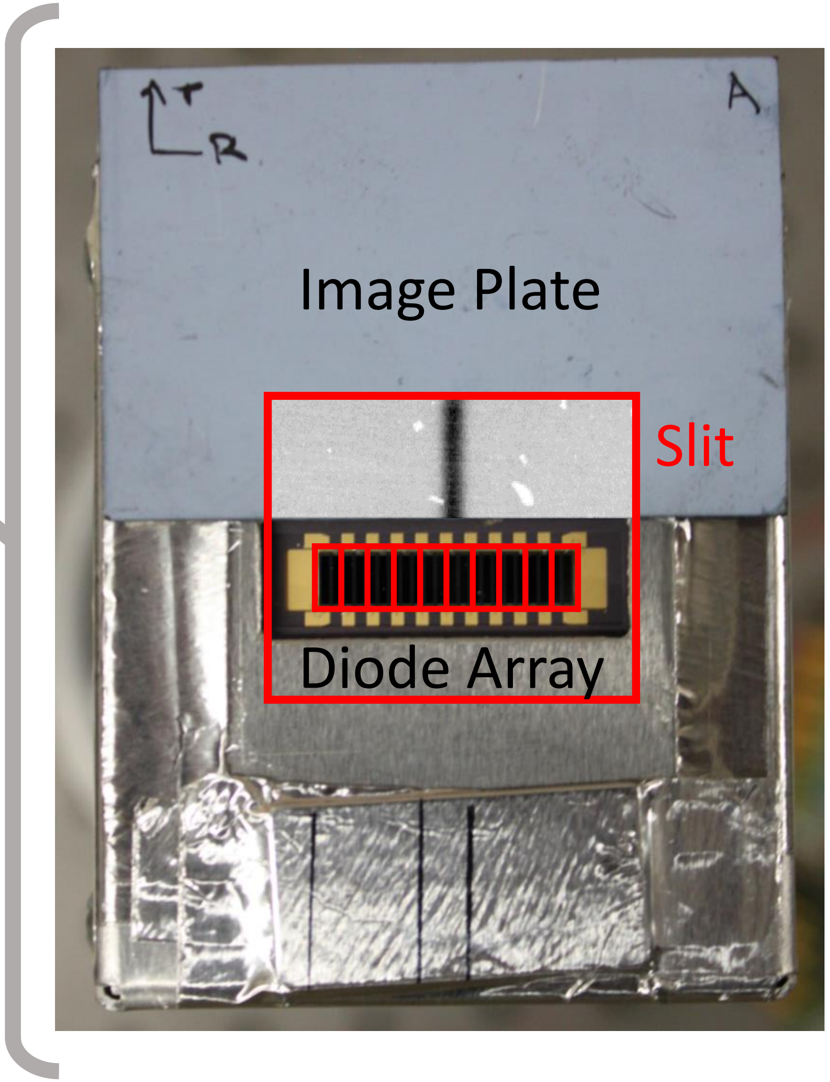

Time Resolved X-Ray Imaging Data

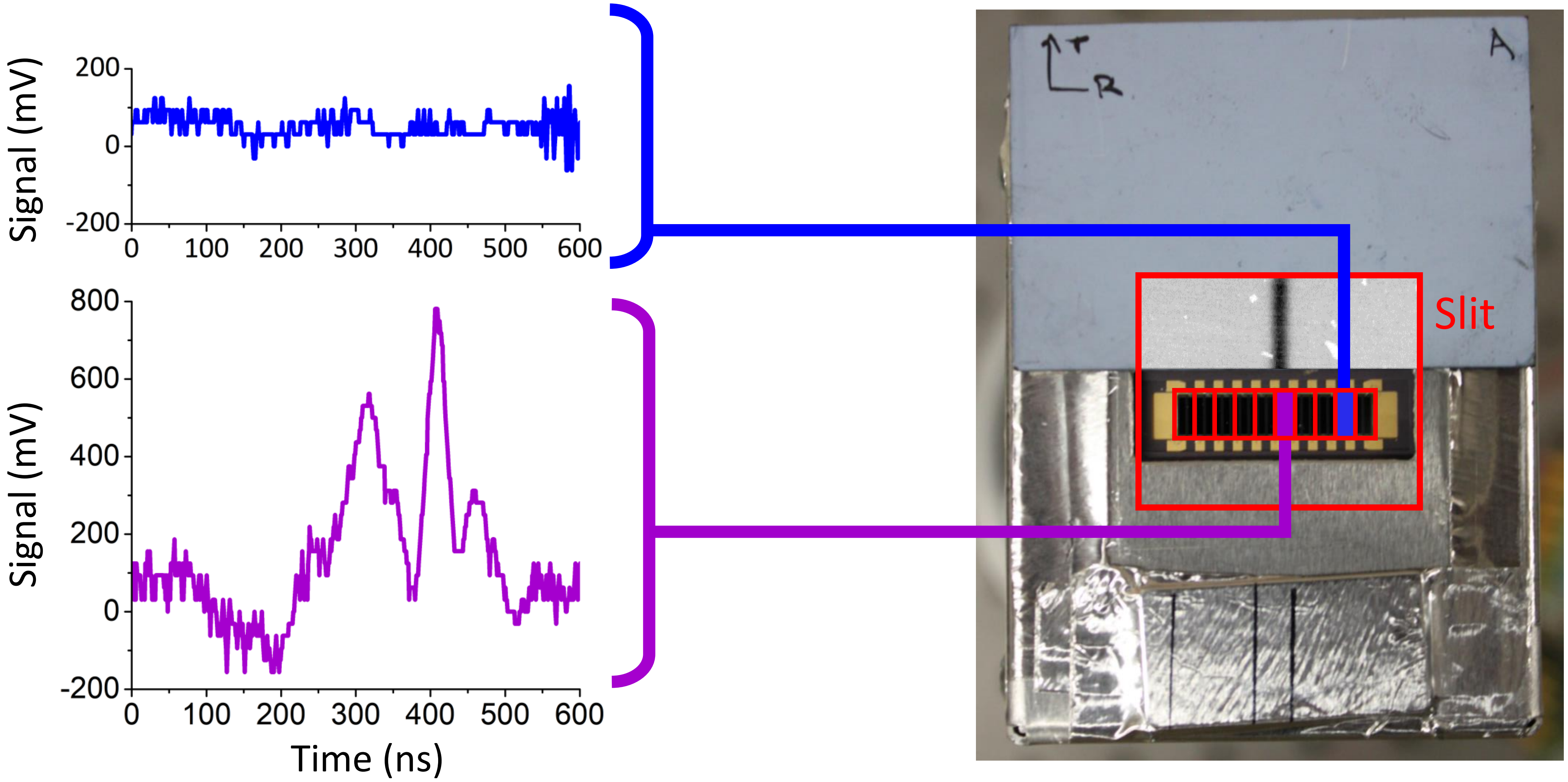

Time Resolved X-Ray Imaging Data

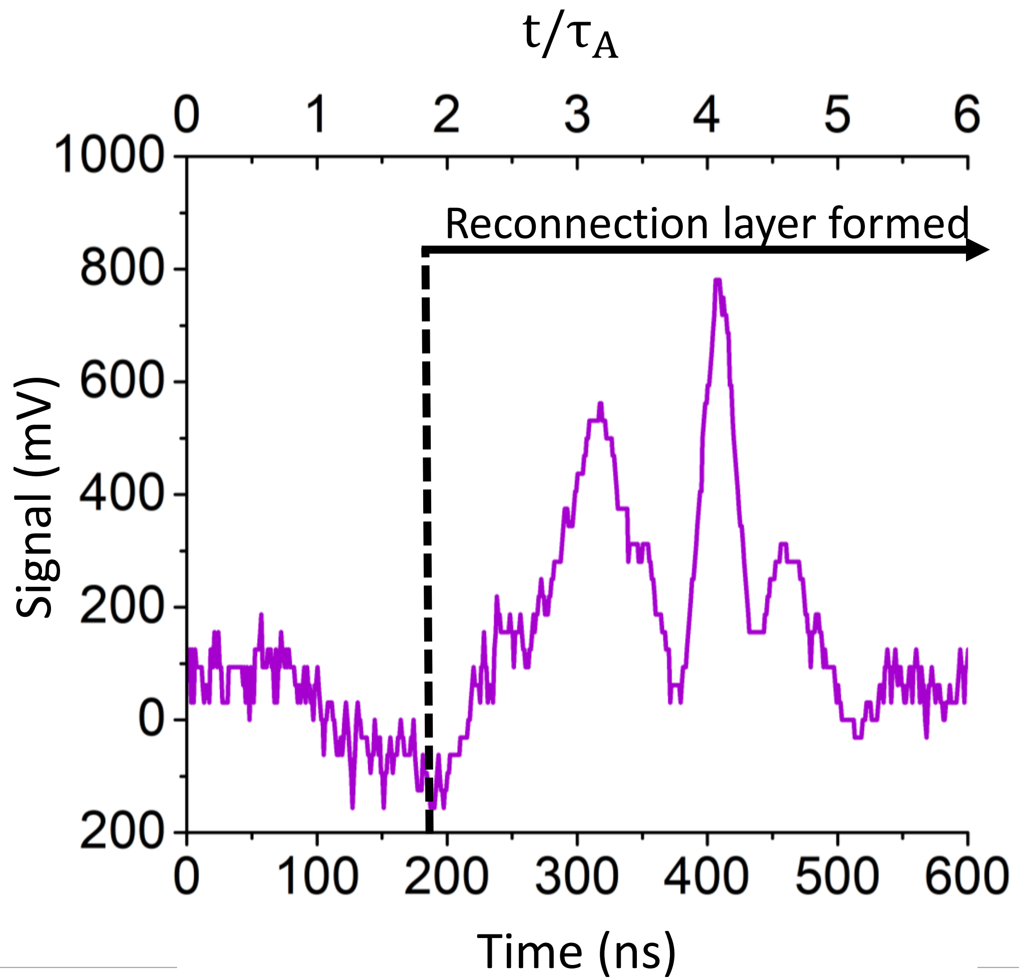

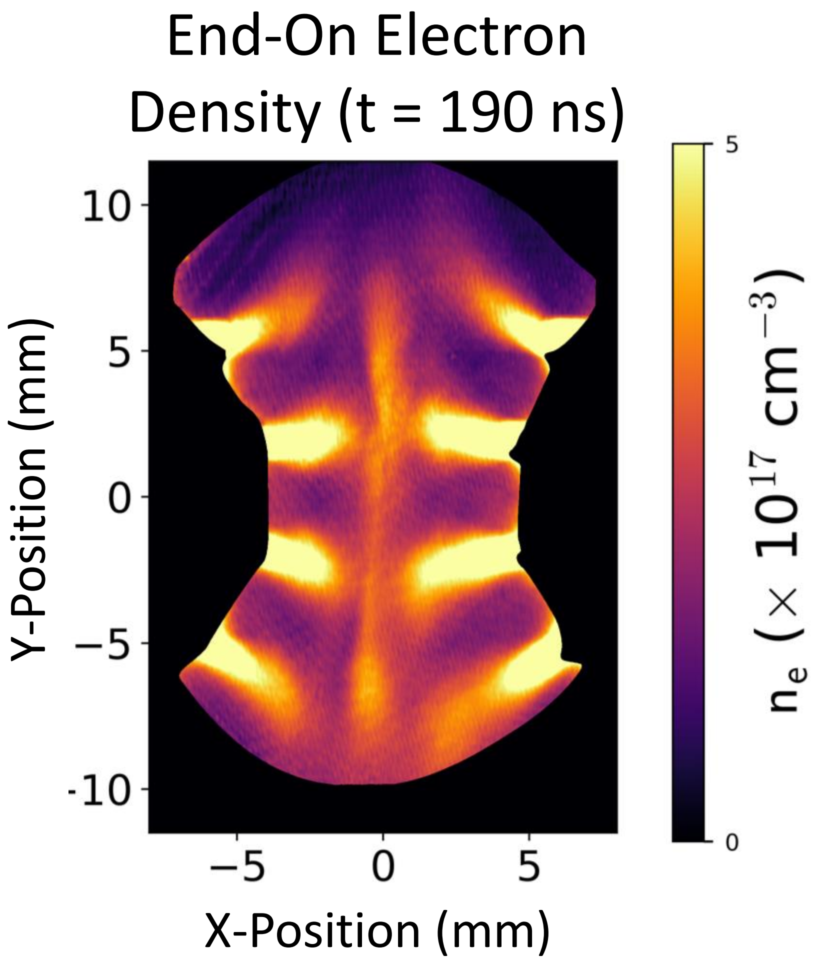

Bursty X-Ray Emission

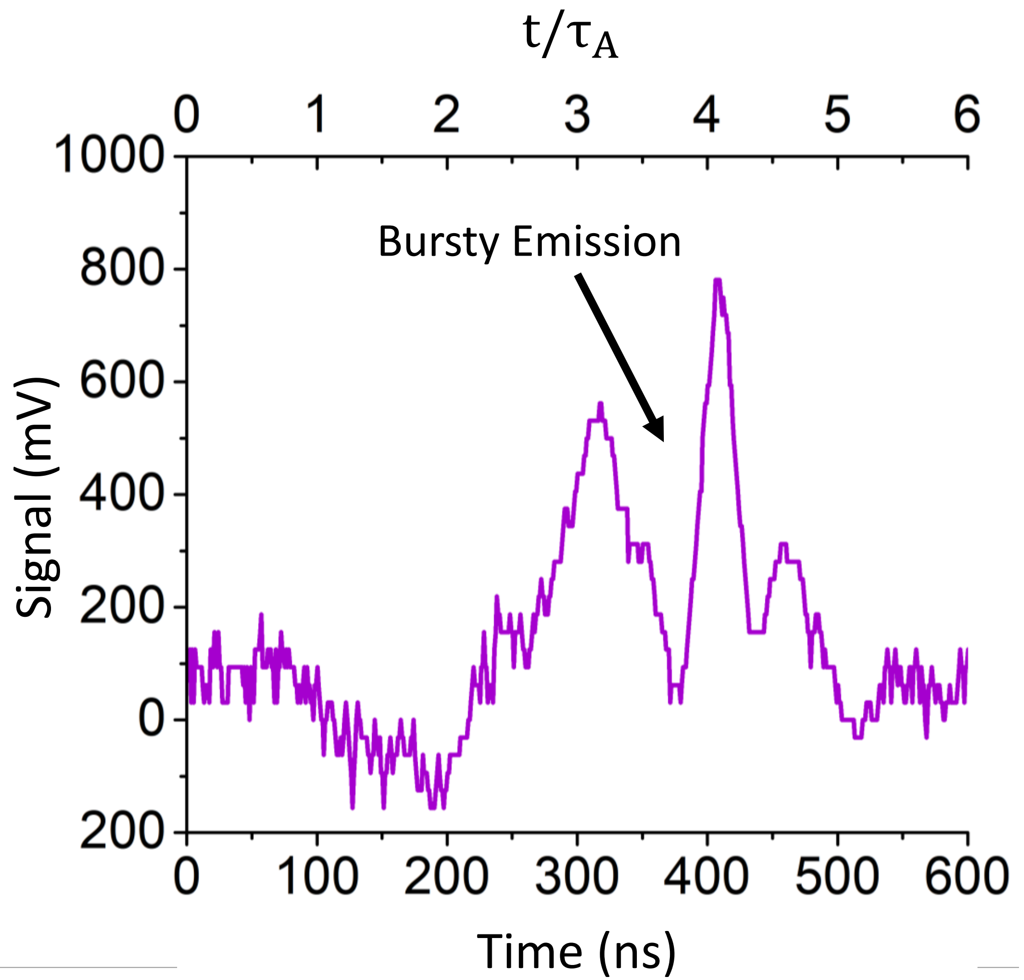

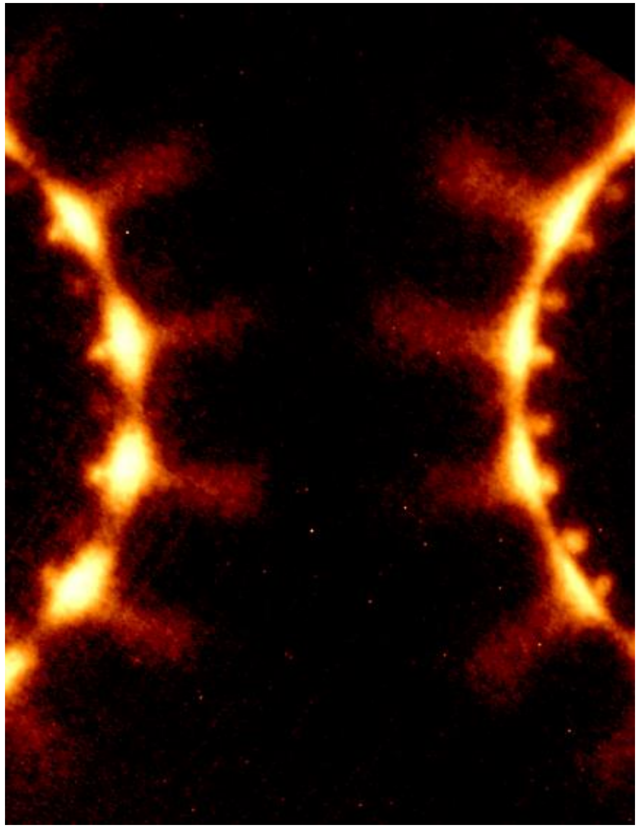

Collisionality in the Reconnection Layer

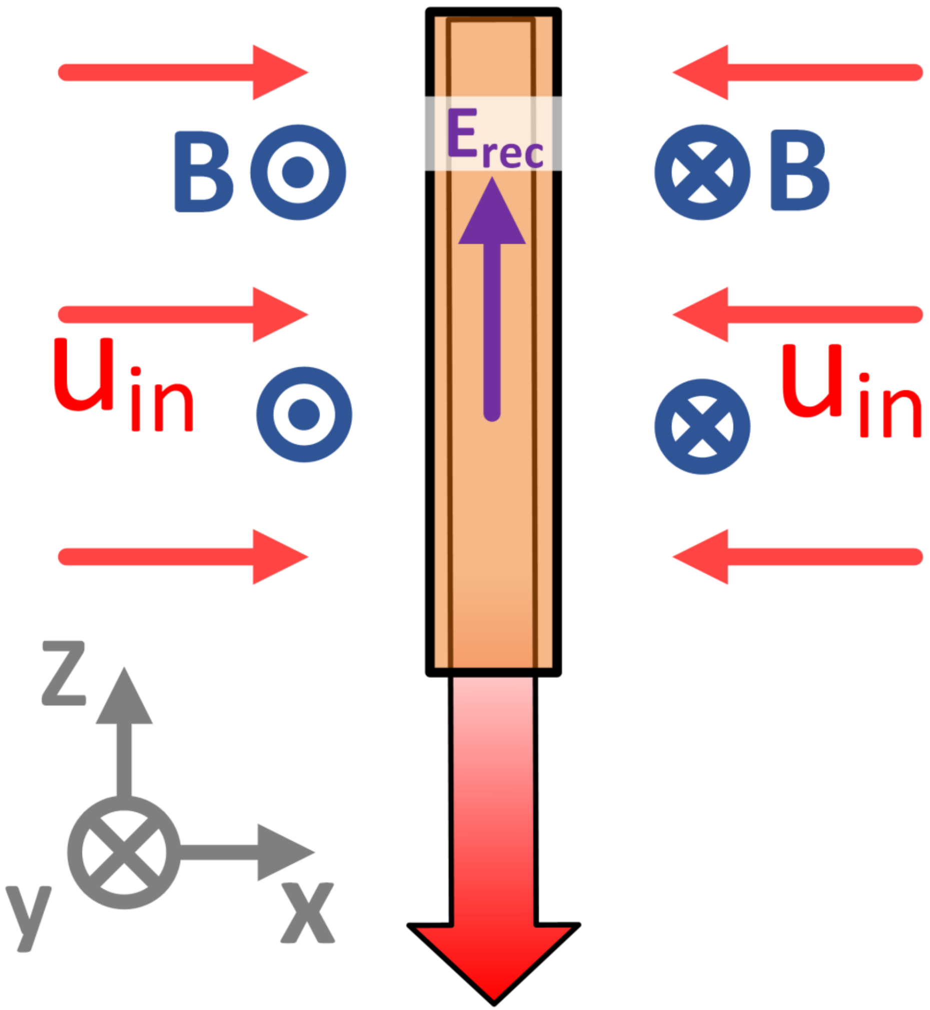

$$\frac{\lambda_{ei}{}^{fast}}{L_Z} \sim 1$$

$$\frac{\lambda_{ei}{}^{\text{thermal}}}{L_z} \sim 10^{-2}$$

$$\frac{E_{rec}}{E_D} \sim 10^{-2}$$

Conclusions

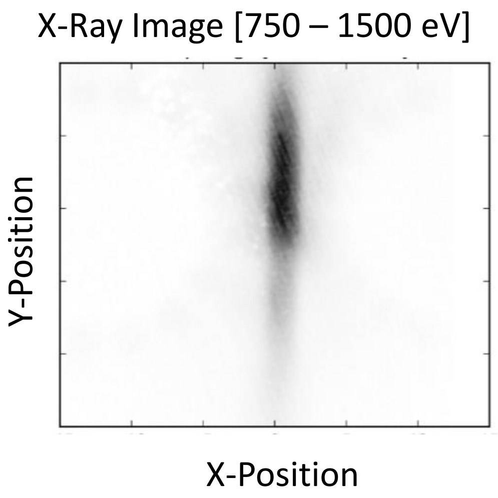

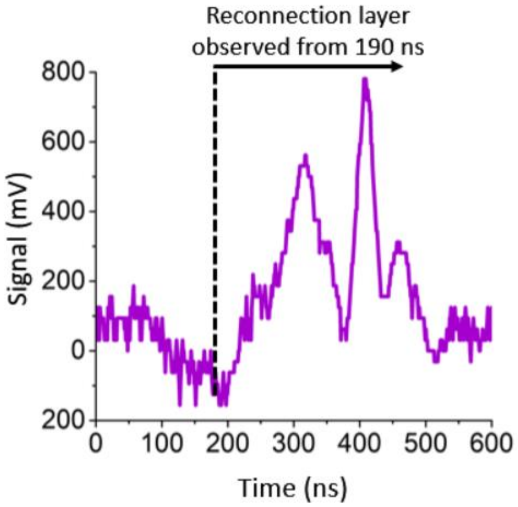

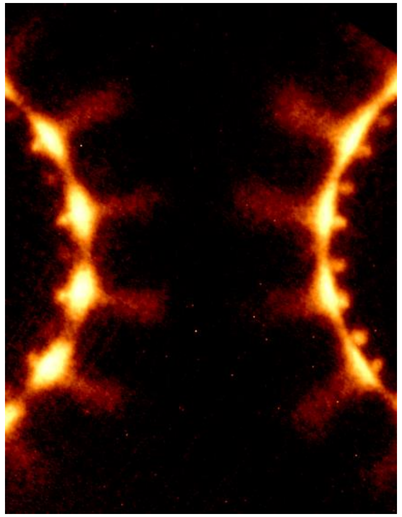

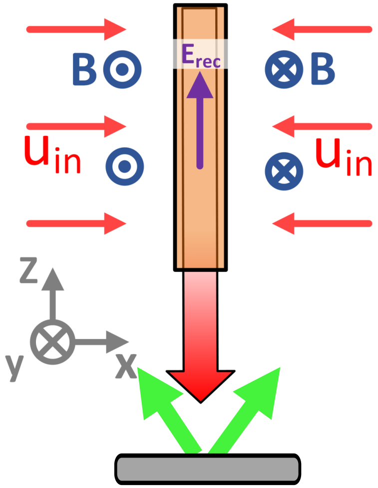

- Reconnection accelerates electrons to energies over 2 keV
- Consistent with acceleration by the reconnecting electric field
- Acceleration bursty ⇒ non steady-state / current sheet instability?

(Relevant simulations: S. Totorica, J07.00009 – 3:35pm in this session)

Supported by EPSRC Grant No. EP/N013379/1, and by the US DOE Awards No. DE-F03-02NA00057, DE-SC-0001063, and DE-NA-0003764.

Plasma Parameters

Parameter	Inflow	Layer
Electron Density (n_e)	3×10^{17} cm^{-3}	6×10^{17} cm^{-3}
Effective Charge ($\bar{Z}$)	4	6
Electron Temp' (T_e)	15 eV	100 eV
Ion Temp' (T_i)	50 eV	600 eV
Layer Half-Length (L)	7 mm	
Layer Half-Width (Δ)	0.6 mm	
Ion skin depth (d_i)	0.71 mm	0.41 mm
Thermal Electron MFP (λ_{ei}^{th})		9×10^{-2} mm
2 keV Electron MFP ($\lambda_{ei}^{\text{fast}}$)		40 mm
Velocity ($\boldsymbol{v}$)	$50\hat{\boldsymbol{x}}$ km/s	$130\hat{\boldsymbol{y}}$ km/s
Alfven Speed (v_A)	70 km/s	…
Sound Speed (C_S)	30 km/s	85 km/s
Fast MS Speed (v_{fms})	75 km/s	…

Parameter	Inflow	Layer
Alfven Time (τ_A)	100 ns	…
Ion-Elec' Cooling Time ($\tau_{e\backslash i}^{E}$)	30 ns	140 ns
Radiative Cooling Time (τ_{rad})	100 ns	600 ns
Magnetic Field (B_y)	3 T	…
Reconnecting E Field (E_{Rec})	150 kV/m	
Dreiser E Field (E_D)		2×10^3 kV/m
Thermal Beta (β_{th})	0.4	…
Dynamic Beta (β_{dyn})	1	…
Lundquist Number (S)	100	
Two-Fluid Effects (L/d_i)		18
$\lambda_{ei}^{\text{th}}/L$		1×10^{-2}
$\lambda_{ei}^{\text{fast}}/L$		1
E_{rec}/E_D		4×10^{-2}

X-Ray Spectroscopy

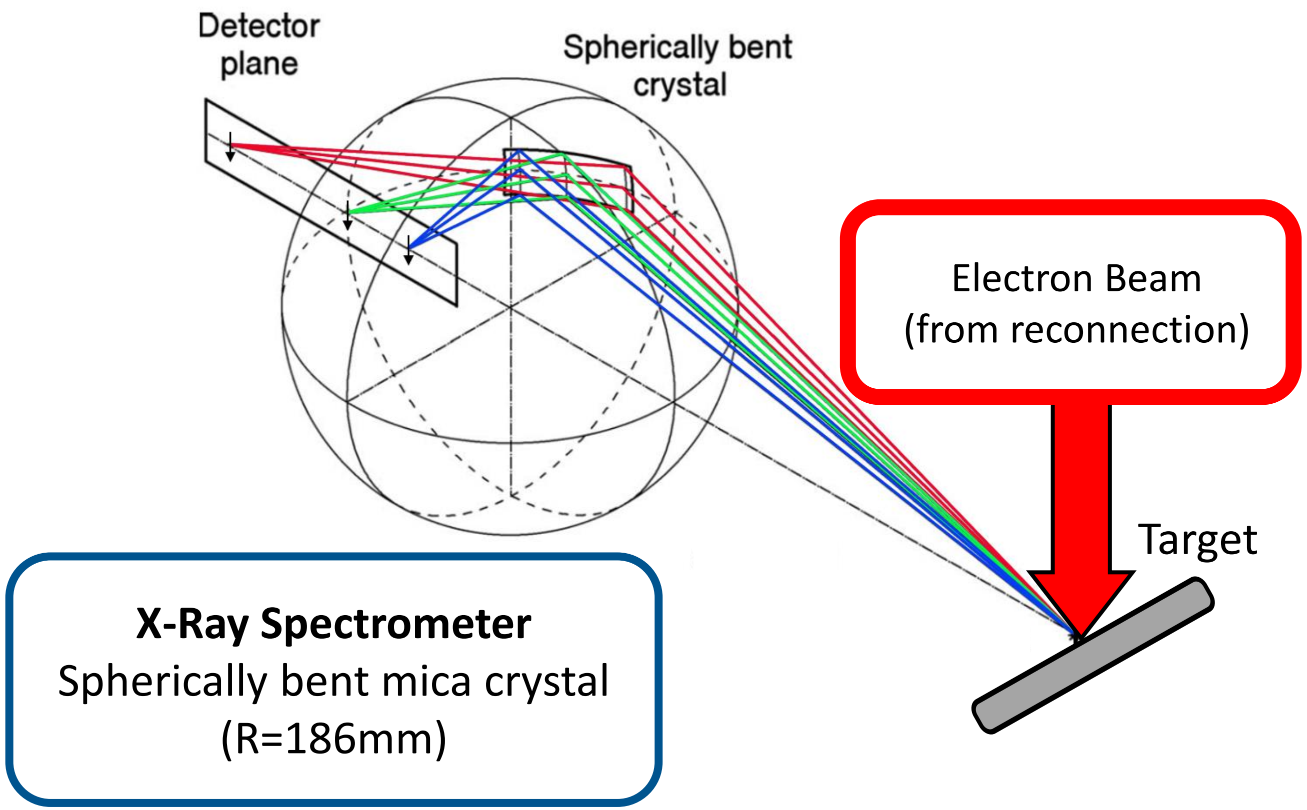

(Adapted from S. A. Pikuz et al. 2008. Rev Sci Instr. 79, 013106)

Time Integrated X-Ray Spectra

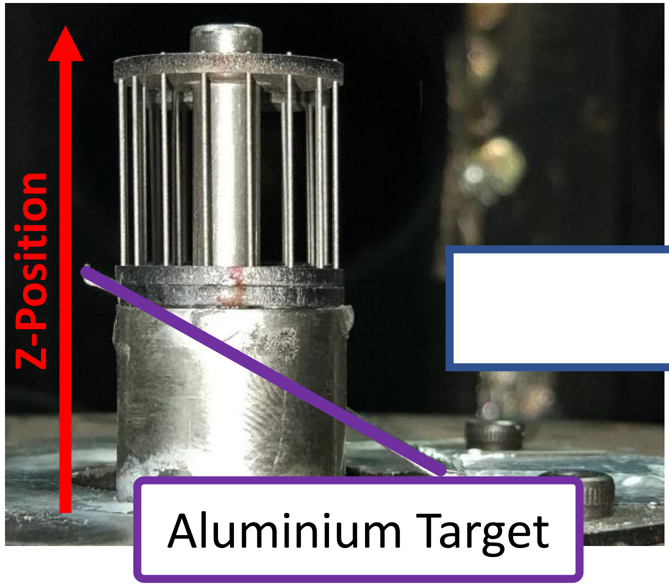

X-Ray Emission (from target)

Spherically Bent Crystal Spectrometer

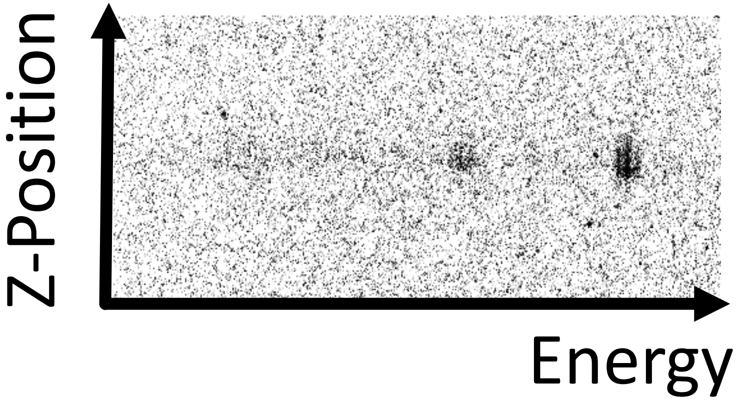

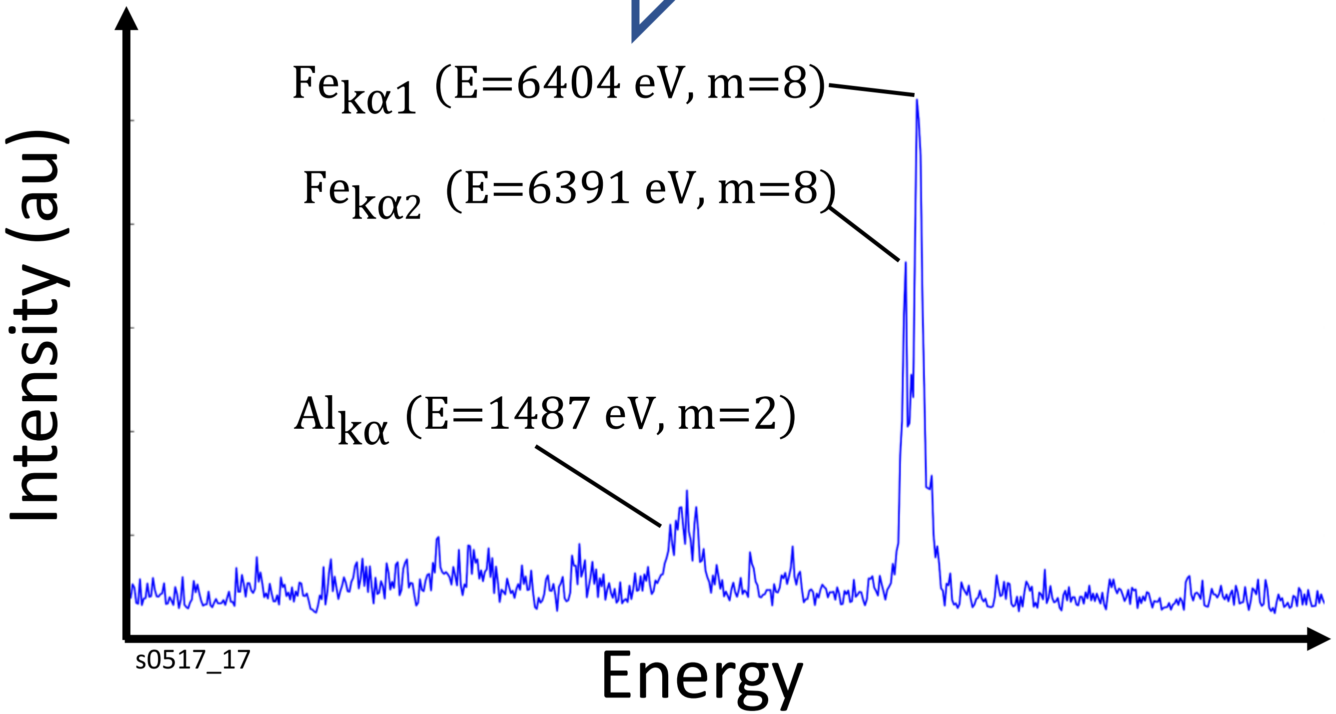

Diagnosing Plasma Flows

Interferometry	Thomson scattering	Faraday-Rotation Imaging
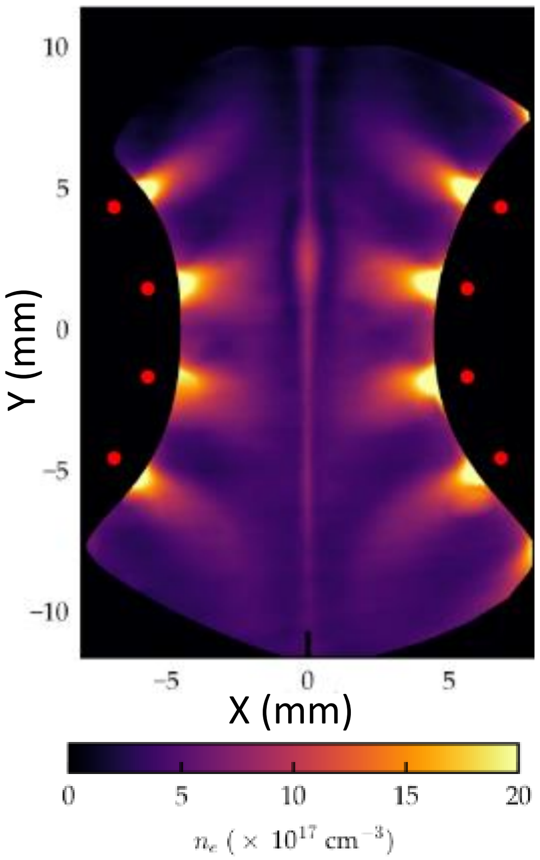	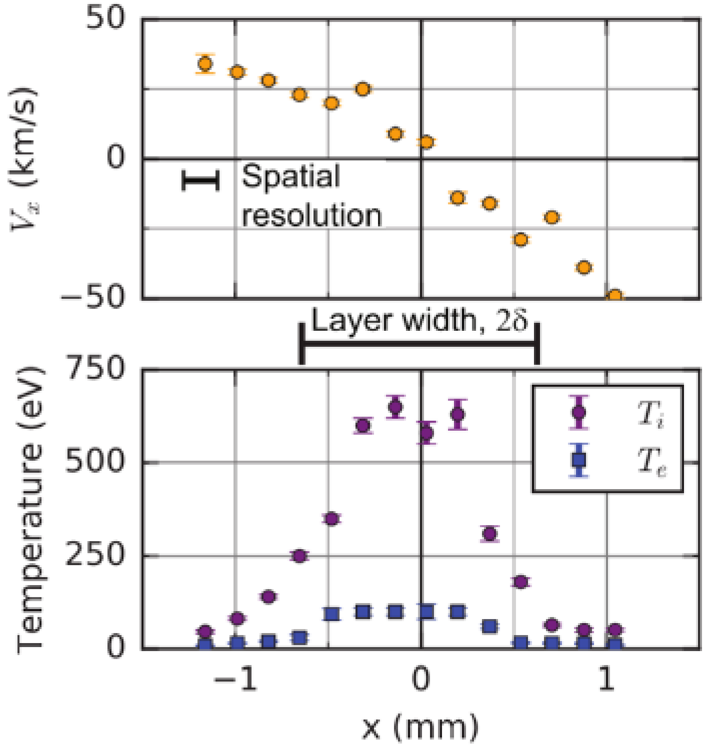	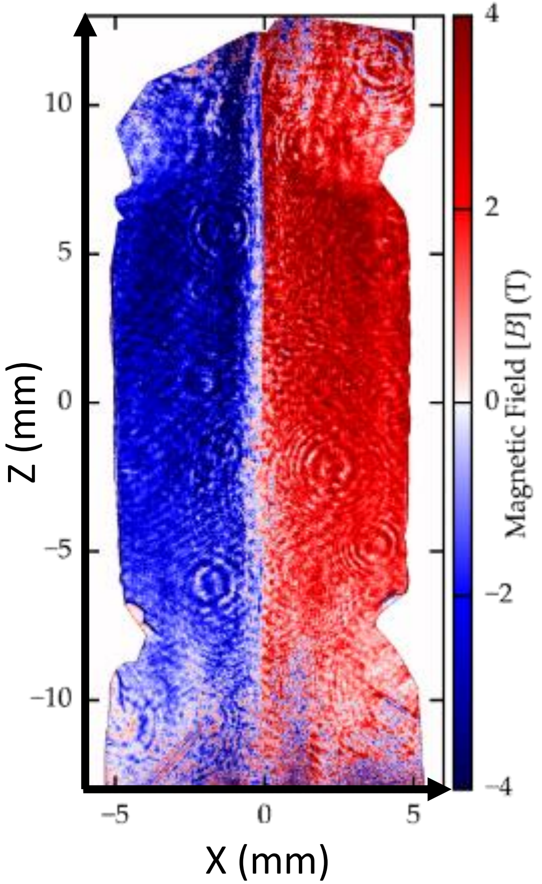

Time Integrated Pinhole Imaging

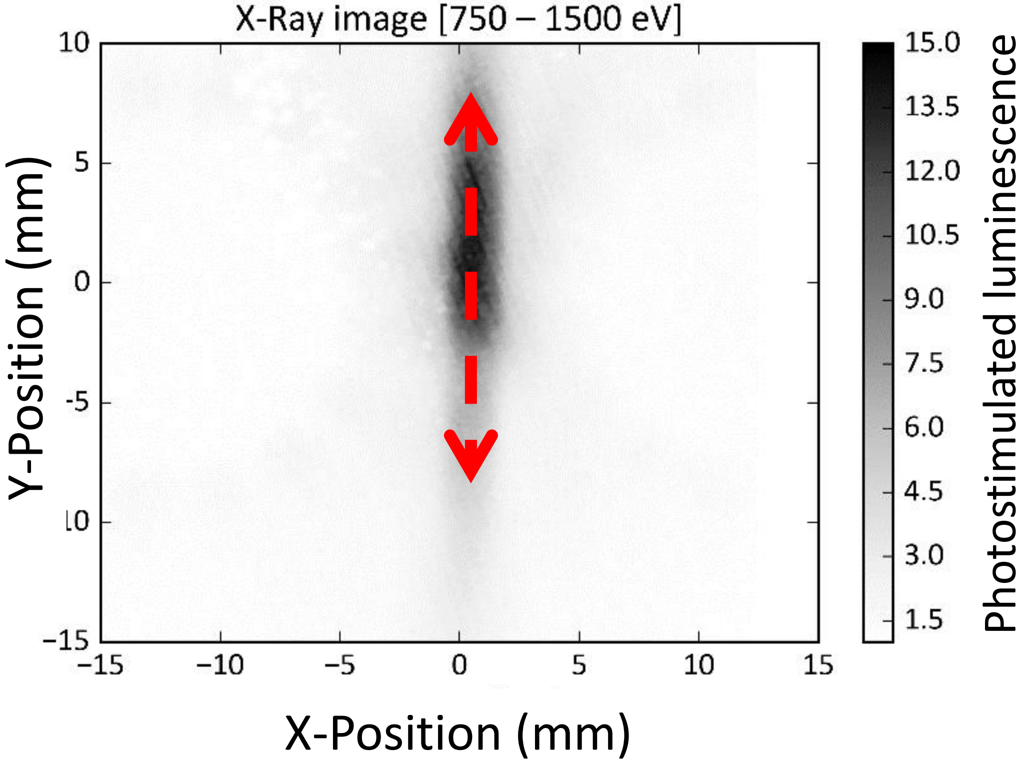

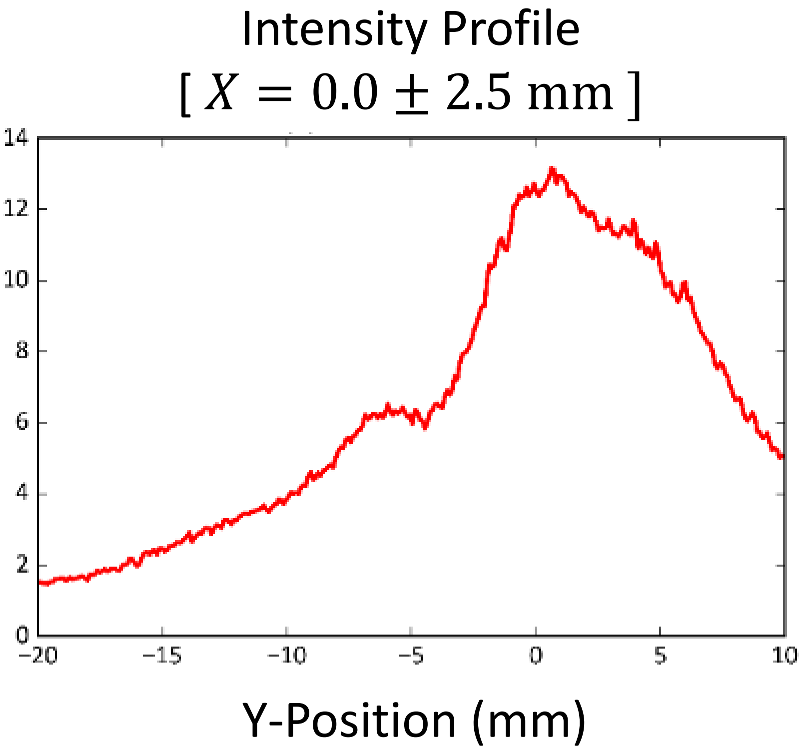

Polypropylene filter transition

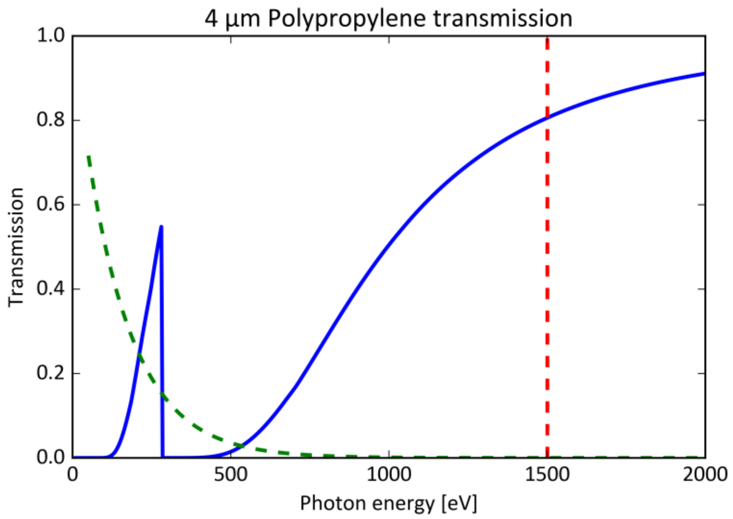

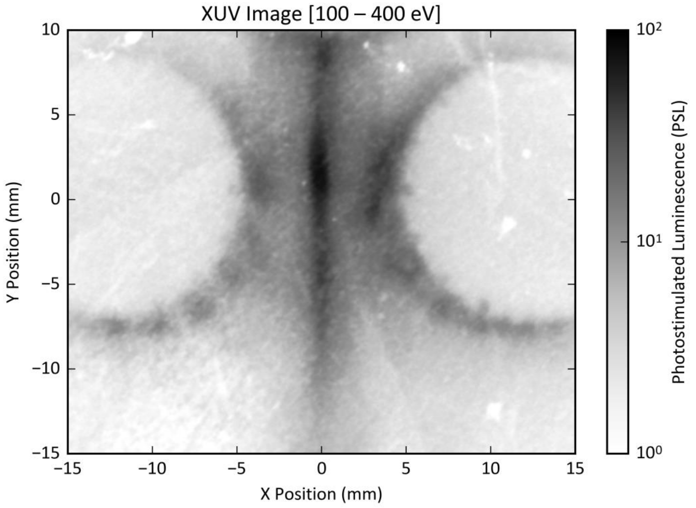

Aluminium filter transition

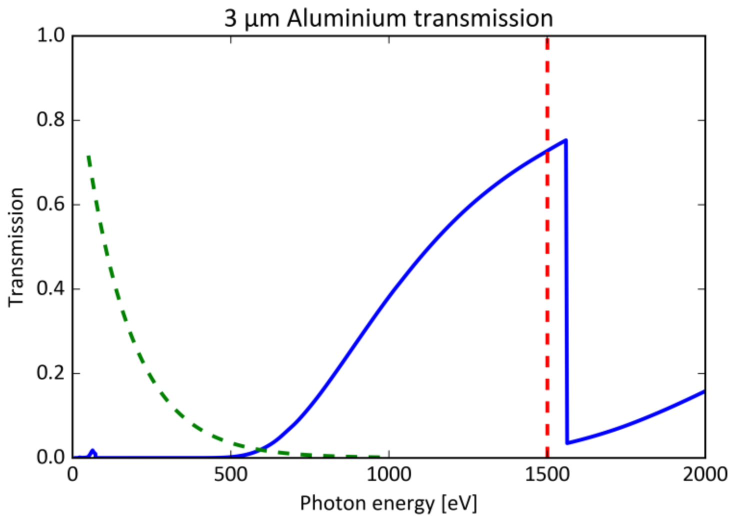

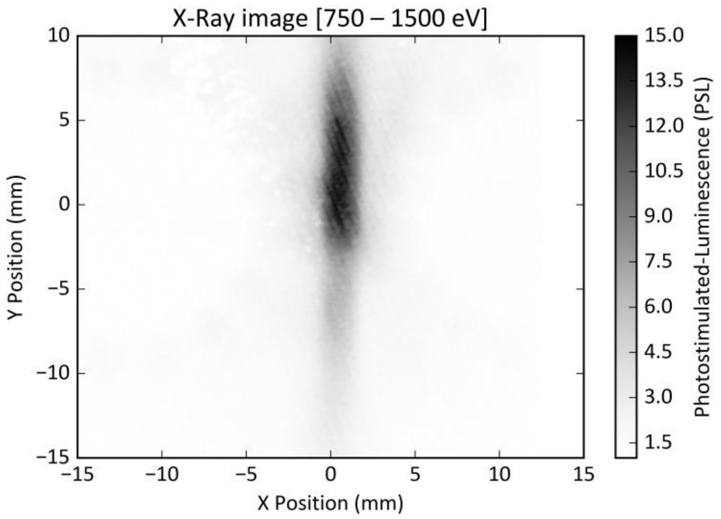

jack.halliday12@imperial.ac.uk

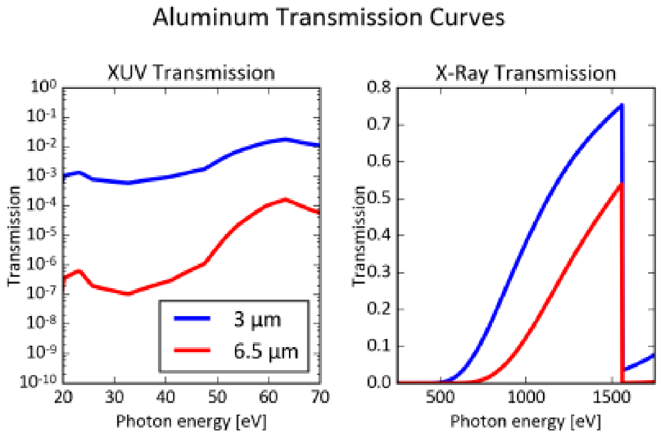

Figure 4.8: Comparison of the transmission spectra of aluminium foils with thicknesses of 6.5 µm and 3 µm, for XUV and X-Ray energies.

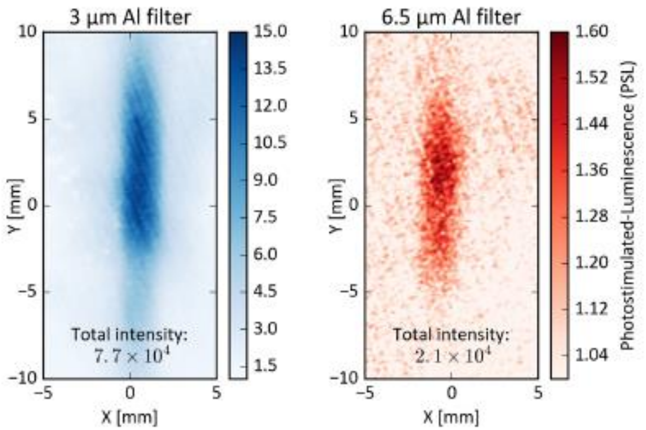

Figure 4.9: End on pinhole images obtained in the same shot (s1016_17) using 800 µm pinholes and two different filters (*blue*- 3 µm aluminium; *red*- 6.5 µm aluminium).

Magnetic Field Profile (Faraday Rotation Imaging)

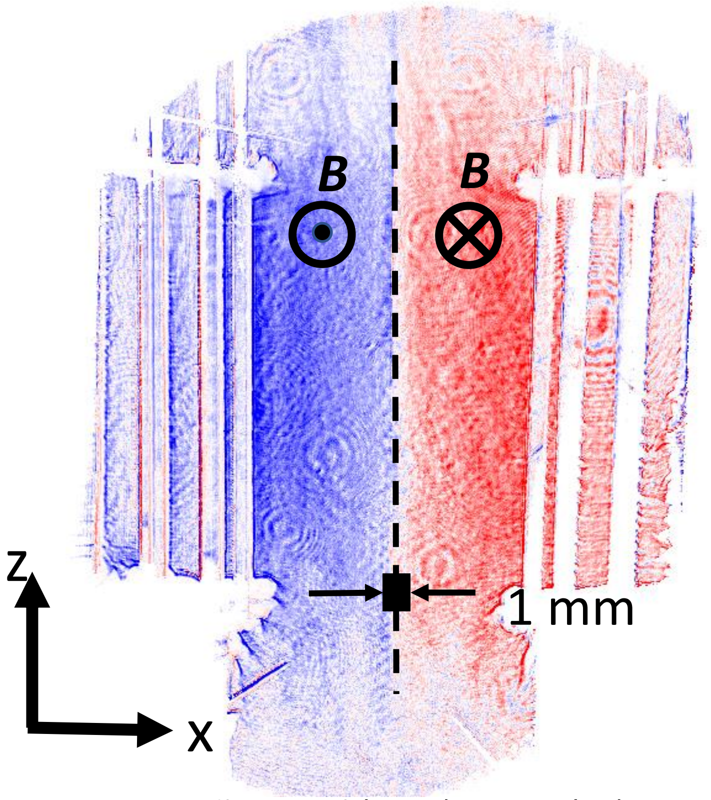

G. F. Swadling et al.(2014). RSI **85** (11), 11E502

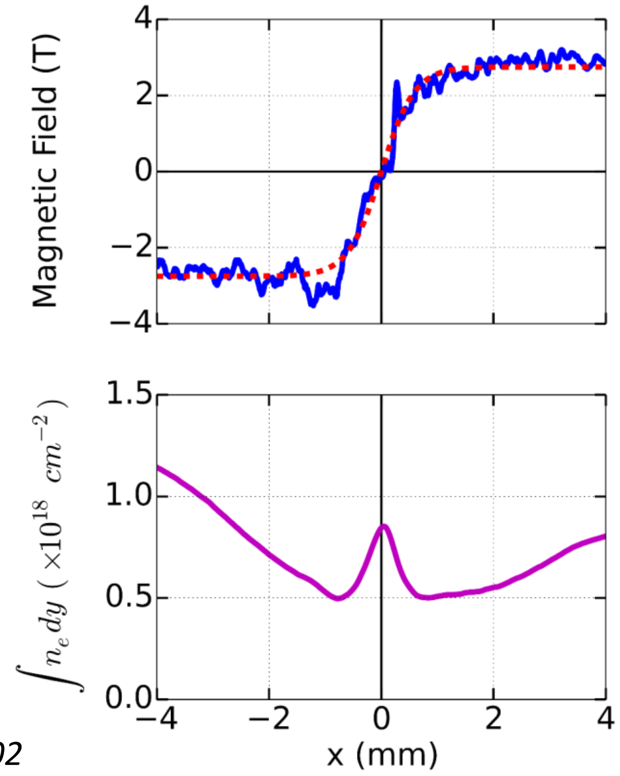

$$\alpha(y,z) \propto \int n_e \boldsymbol{B}.d\boldsymbol{x}$$

Harris Sheet:

$$B = B_0 \tanh(x/\delta)$$

$$B_0 = 3\,\mathrm{T}$$

$$\delta = 0.6\,\mathrm{mm}$$

Velocity and Temperature (Thomson Scattering)

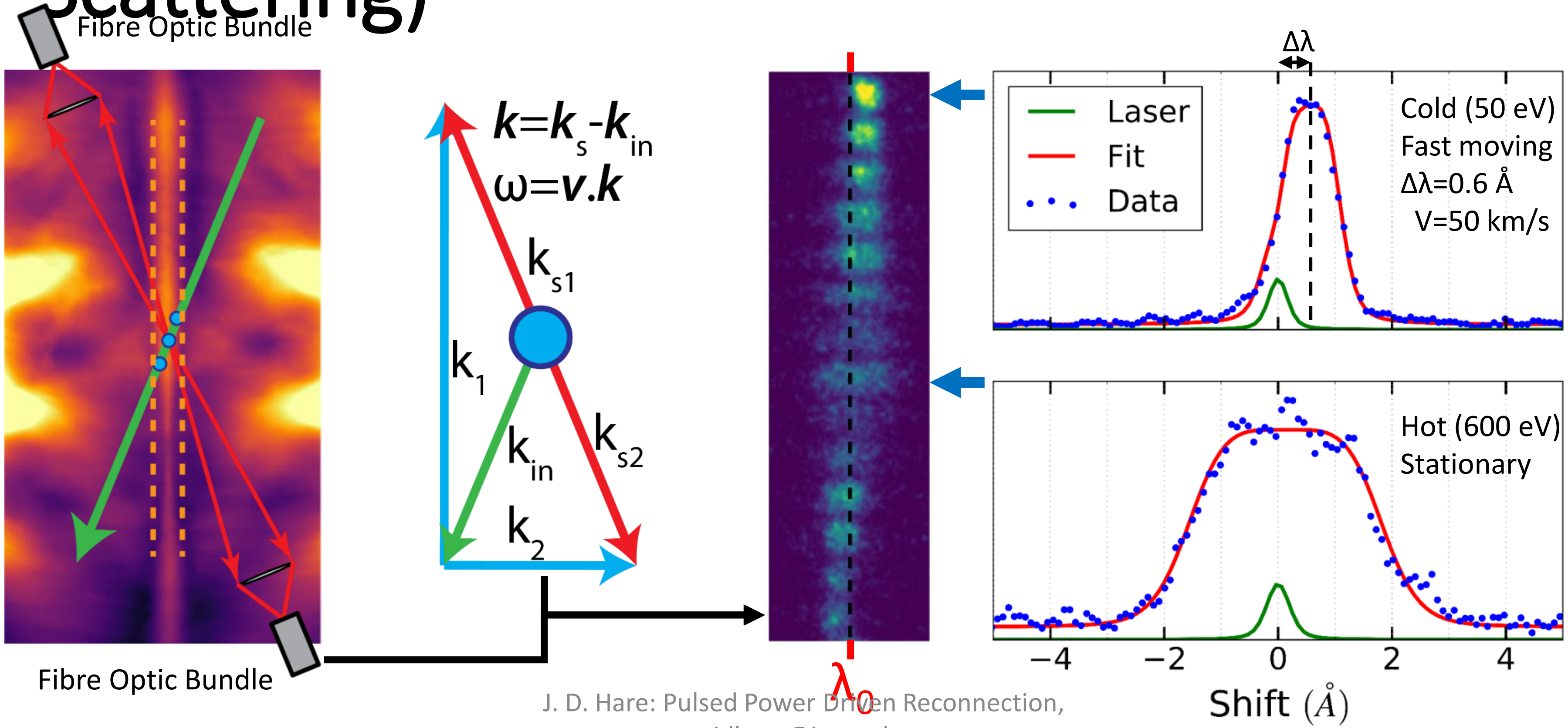

Post-shot images of target

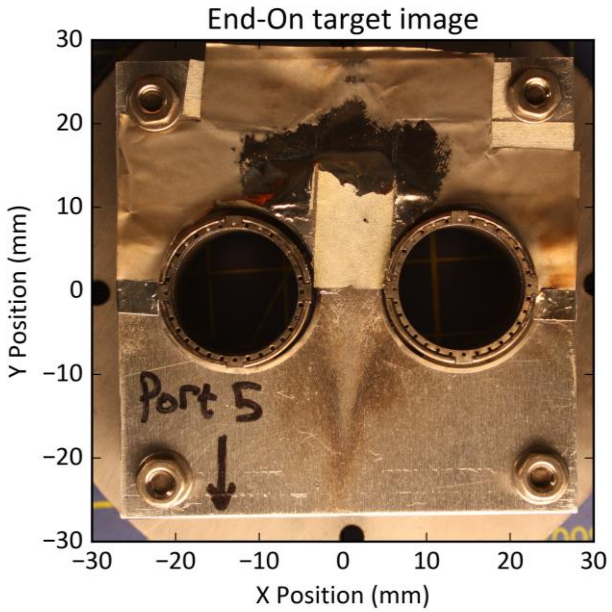

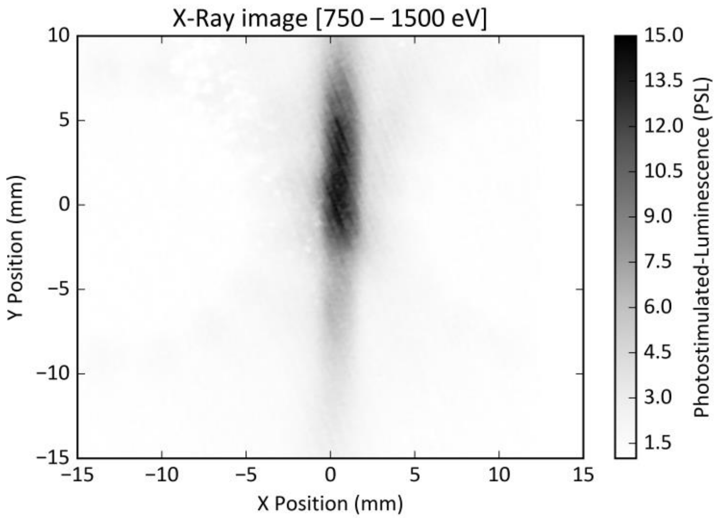

jack.halliday12@imperial.ac.uk

Ionisation cross section

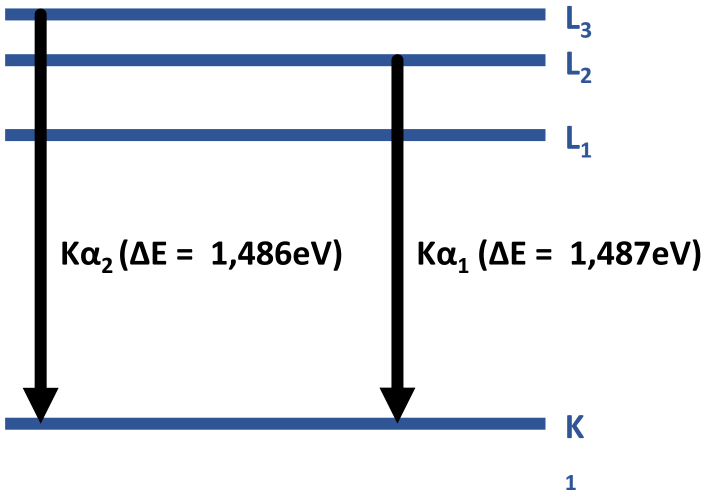

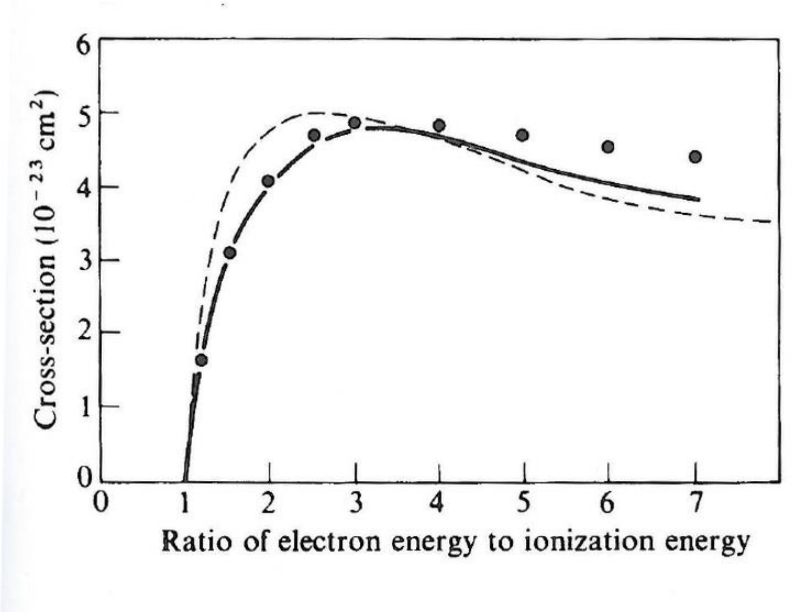

Ref: Dyson, N. A. (2009) X-Rays in atomic and nuclear physics